Strong postmating reproductive isolation in *Mimulus* section *Eunanus*

Matthew C. Farnitano[1]*, Andrea L. Sweigart[1]

[1]Department of Genetics, University of Georgia, Athens, GA, 30602, USA.

*Corresponding author:

Matthew Farnitano

120 W. Green St

Athens, GA 30602

mattfarnitano@gmail.com

ABSTRACT

Postmating reproductive isolation can help maintain species boundaries when premating barriers to reproduction are incomplete. The strength and identity of postmating reproductive barriers are highly variable among diverging species, leading to questions about their genetic basis and evolutionary drivers. These questions have been tackled in model systems but are less often addressed with broader phylogenetic resolution. In this study we analyze patterns of genetic divergence alongside direct measures of postmating reproductive barriers in an overlooked group within the model monkeyflower genus, *Mimulus*. Within this *Mimulus brevipes* species group, we find substantial divergence among species, including a cryptic genetic lineage. However, rampant gene discordance and ancient signals of introgression suggest a complex history of divergence. In addition, we find multiple strong postmating barriers, including postmating prezygotic isolation, hybrid seed inviability, and hybrid male sterility, leading to complete or substantial postmating isolation in all species pairs. Hybrid seed inviability appears linked to differences in seed size, providing a window into the developmental mechanisms underlying this reproductive barrier. While geographic proximity and incomplete mating isolation may have allowed gene flow within this group in the distant past, strong postmating reproductive barriers today are likely to prevent any ongoing hybridization. By investigating reproductive isolation in a phylogenomic context, we highlight the benefits of understudied species groups to our understanding of speciation.

KEY WORDS: postmating reproductive isolation, introgression, *Mimulus*, hybrid seed inviability, speciation

INTRODUCTION

Evolutionary biologists have long been interested in understanding what patterns and processes lead to reproductive isolation among species (Coyne & Orr, 1997; Darwin, 1859; V. Grant, 1981). Reproductive isolation is often broken down into components that act at sequential stages of the life cycle – premating barriers such as ecogeographic isolation and pollinator-mediated isolation act to prevent mating, postmating prezygotic barriers that reduce fertilization success after mating has occurred, and postmating postzygotic barriers that reduce the fitness of hybrid offspring relative to pure species (Ramsey et al., 2003; Sobel & Chen, 2014). In plants, premating barriers are typically thought to evolve more quickly than postmating barriers and to have a greater contribution to overall isolation (Christie et al., 2022). However, this general pattern masks a great deal of heterogeneity across species pairs: many systems are completely isolated by premating barriers, while others rely exclusively on strong postmating isolation; many have a mix of both. Postmating barriers are often the result of intrinsic genetic incompatibilities, making them potentially more stable over the long term than ecologically mediated premating barriers (Coughlan & Matute, 2020). Postmating barriers may also be a source of cryptic variation in groups without obvious morphological or ecological differences.

To fully understand the role that postmating reproductive barriers play in speciation, they must be placed in a phylogenetic context. The degree of reproductive isolation between two taxa tends to increase with genetic distance (Christie & Strauss, 2018; Coyne & Orr, 1989; Malone & Fontenot, 2008; Scopece et al., 2007), but this relationship is not always consistent across taxa (Moyle et al., 2004) and is highly heterogeneous. In addition, individual

67 reproductive barriers such as sterility and inviability may arise at different rates (Coyne & Orr,
68 1989; Le Gac et al., 2007; Malone & Fontenot, 2008; Presgraves, 2002). The reasons behind
69 these differences are a subject of ongoing investigation, but may include differences in genetic
70 architecture (Guerrero et al., 2017; Moyle & Payseur, 2009) or the forms of selection acting on
71 each barrier (Baack et al., 2015). For example, conflicting selection pressures between maternal
72 and paternal genomes in the mammalian placenta or the flowering plant endosperm are
73 thought to give rise to reproductive barriers as these conflicts are resolved differently in
74 independent lineages (Crespi & Nosil, 2013; Haig & Westoby, 1991; Lafon-Placette & Köhler,
75 2016); the relative strength of this parental conflict could influence the rate of barrier evolution
76 (Coughlan et al., 2020; Raunsgard et al., 2018).

77 An excellent system for building a phylogenetically informed understanding of
78 reproductive isolation is the western North American radiation of monkeyflowers in the genus
79 *Mimulus.* Multiple species groups within *Mimulus* have already been studied extensively in a
80 speciation context, including the *Mimulus guttatus* (e.g., Brandvain et al., 2014; Ferris et al.,
81 2014; Lowry & Willis, 2010), *M. aurantiacus* (e.g., Stankowski et al., 2019; Streisfeld & Kohn,
82 2005), and *M. lewisii* (e.g., Nelson et al., 2021; Ramsey et al., 2003) species complexes. A
83 number of pre- and postmating reproductive barriers have been mapped to single genes or QTL
84 (e.g., Fishman et al., 2014; Fishman & Willis, 2006; Streisfeld & Rausher, 2009; Sweigart et al.,
85 2006; Yuan et al., 2013; Zuellig & Sweigart, 2018). Recently, hybrid seed inviability in particular
86 has been identified as a strong barrier in multiple independent species pairs of the *Mimulus*
87 *guttatus* species complex, with parental conflict repeatedly implicated as a common
88 mechanism (Coughlan et al., 2020; Oneal et al., 2016; Sandstedt et al., 2020; Sandstedt &

Sweigart, 2022). An expanding trove of genetic and developmental resources across the genus allow for a holistic approach to understanding reproductive isolation from genic to phylogenetic scales (Yuan, 2019).

However, some *Mimulus* subgroups have received less attention, in part because they are less experimentally tractable or more difficult to access. One such neglected group is *Mimulus* section *Eunanus* [synonym *Diplacus* section *Eunanus,* see (Barker et al., 2012; Lowry et al., 2019) for a discussion of nomenclatural issues]. Section *Eunanus* is a clade of ~23 species (A. L. Grant, 1924; Nesom, 2013) which prior to this publication has had no genome-scale sequencing and few assessments of reproductive isolation. The group includes both widespread and narrowly endemic species occupying a range of elevations and habitats in western North America. Here, we focus primarily on three species from this group: *Mimulus brevipes* Benth.*, Mimulus fremontii* (Benth.) Gray*, and Mimulus johnstonii* Grant (Baldwin et al., 2012; A. L. Grant, 1924). These three morphologically defined species make up a well-supported clade according to a phylogenetic study of *Mimulus* based on three genetic markers (Beardsley et al., 2004). Their ranges are overlapping; *M. johnstonii* is restricted to higher elevations in the Transverse Ranges of southern California, while *M. fremontii* and *M. brevipes* are more widespread throughout the coastal ranges from Monterey into Baja California (Figure 1B).

Studies of reproductive isolation in these three species are limited. Species distribution modeling between *Mimulus johnstonii* and *M. brevipes* identified strong but incomplete ecogeographical isolation (RI=0.65 and 0.82 reciprocally) (Sobel, 2014), and they can be found within hundreds of feet of each other (pers. obs.). No distribution models have been made with *M. fremontii*, but M*. brevipes* and *M. fremontii* are found at similar elevations, flower at similar

111 times, and can be found growing within inches of each other (pers. obs.). Major differences in
112 flower color, size, and shape between *M. brevipes* and its relatives might suggest some degree
113 of pollinator-mediated isolation, though little is known about the identity of pollinators or
114 levels of outcrossing; *M. fremontii* and *M. johnstonii* have similar floral characteristics and seem
115 unlikely to have substantial pollinator isolation. Postmating barriers have not been studied,
116 with the exception of one study showing low germination rates of F1 hybrid seeds between *M.*
117 *brevipes* and *M. johnstonii,* potentially suggesting hybrid seed inviability (Sobel, 2010).
118 In this study, we present the first genome-scale analysis of divergence relationships in
119 *Mimulus* section *Eunanus*, incorporating our three focal species as well as two more distant
120 species, *M. constrictus* and *M. nanus*. In addition, we use controlled crosses to examine
121 multiple postmating reproductive barriers between the focal species. We find clear genetic
122 divergence and multiple strong postmating reproductive barriers between all tested species.
123 Our results add to a growing body of evidence that intrinsic postmating barriers, especially
124 hybrid seed inviability, are a key component in the maintenance of plant species.
125

126 **MATERIALS AND METHODS**

127 *Sample collections and growth conditions*

128 Fruits were collected from wild plants of three focal species (*M. brevipes, M. fremontii,*
129 and *M. johnstonii*) at nine locations in southern California in summer 2019 (Figure 1B, Table S1).
130 As additional, more phylogenetically distant comparisons, a population of *M. nanus* in Oregon
131 and a population of *M. constrictus* from California were collected in 2021. To germinate, we
132 treated seeds overnight with 1 mM giberrellic acid, then rinsed three times with distilled water

133 and placed them individually in 2x2cm soil plugs. Soil was a 1:1:1 mix of sand, perlite, and peat
134 with a thin layer of finely sifted soil mix on top. Germination trays were set in standing bottom
135 water and kept moist with a squirt bottle as necessary. When germination rates were low,
136 liquid smoke was added to standing water to simulate post-fire conditions and stimulate
137 germination. After germinants developed one or two pairs of true leaves, we transplanted soil
138 plugs into plastic conical pots filled with the same soil mix. The conical pots were maintained in
139 standing bottom water in a growth chamber set to 23C days/18C nights, with low relative
140 humidity and 16 hours of daylight.

141 One population initially collected as *M. johnstonii,* S25 from Sespe Creek, showed
142 morphological differences suggesting it may be a unique lineage, and is treated separately
143 throughout this paper. Compared to *M. johnstonii*, Sespe Creek has inserted stigmas, a lighter
144 purple corolla with a slight white wash at the mouth, and longer leaf trichomes.

145

146 *Genomic sequencing*

147 We collected leaf tissue from 33 individuals for genomic sequencing. All sequenced
148 individuals were generated from outbred field-collected seeds and germinated in growth
149 chambers. We flash-froze leaf tissue in liquid nitrogen and used a modified CTAB-based
150 protocol to extract genomic DNA (Fishman, 2020). Briefly, tissue was ground to a powder and
151 incubated in CTAB buffer with ß-mercaptoethanol. Supernatant was extracted with phenol-
152 chloroform-isoamyl alcohol, then again with chloroform-isoamyl alcohol, followed by
153 precipitation of carbohydrates with sodium chloride and polyethylene glycol. DNA was then
154 precipitated with isopropanol, washed with ethanol, and resuspended in distilled water.

155 We used the tagmentation-based Illumina Nextera XT DNA library prep kit (FC-131-1024)
156 to prepare genomic DNA for sequencing. The 33 individually barcoded samples were then
157 sequenced in four batches at the Duke University Sequencing and Genomic Technologies
158 Shared Resource with either an Illumina NextSeq 500 or an Illumina NovaSeq 6000 sequencer,
159 in combined lanes with other barcoded projects (Table S2).

160 *Sequence alignments and SNP calling*

161 We combined our dataset of 33 samples with five previously published samples
162 (Stankowski et al., 2019) from the *Mimulus aurantiacus* species complex for analysis. For all 38
163 samples, we trimmed raw sequencing reads using Trimmomatic v0.39 (Bolger et al., 2014) to
164 remove adapters and low-quality ends. We mapped reads to the *Mimulus aurantiacus*
165 reference genome (Stankowski et al., 2019) using bwa mem v0.7.17 (Li & Durbin, 2009), then
166 sorted and indexed with samtools v1.10 (Danecek et al., 2021). We removed PCR duplicates
167 using the MarkDuplicates tool in Picard v2.21.6 (Broad Institute, 2019), and removed reads
168 with unmapped mate pairs or mapping quality <29 using samtools view (Danecek et al.,
169 2021). No genome assembly currently exists for *Mimulus* section *Eunanus*, so *M. aurantiacus* is
170 the closest available reference genome.

171 We called SNPs in each sample using the GATK v4.1.6.0 haplotype caller, then used GATK
172 GenotypeGVCFs to jointly call variant and invariant sites for the entire dataset in 'all-sites'
173 mode (Van der Auwera & O'Connor, 2020). We split the resulting VCF into SNPs and invariant
174 sites, and separately filtered each before recombining them into a joint dataset, following
175 recommendations by Dmitri Kryvokhyza (Kryvokhyzha, n.d.). We filtered both SNPs and
176 invariant sites to remove sites with combined DP <83 (~1/3 of mean combined depth) or >1376

177 (two standard deviations above mean combined depth), QD<2, SOR>3, or MQ<40. We
178 additionally filtered SNPs to keep only biallelic sites across the entire dataset, and to remove
179 sites with QUAL<40, FS>60, MQRankSum<-12.5, ReadPosRankSum>12.5, or ReadPosRankSum<-
180 12.5.

181 We used four datasets of variants for downstream analyses. A 'filtered' dataset included
182 all sites that pass the above filters, resulting in 14,814,282 biallelic SNPs and 96,871,941
183 invariant sites. An '80% called' dataset further removed any site where fewer than 30 of 38
184 (approximately 80%) of samples had a called genotype, retaining 7,728,322 biallelic SNPs
185 and 32,658,171 invariant sites. Next, our 'downsampled' dataset attempted to reduce bias due
186 to uneven sampling of species and uneven coverage across individuals. We chose two
187 individuals per species (except for *M. constrictus* for which we only had one sample), then
188 randomly sampled 12 million raw read pairs from each individual and used the same pipeline as
189 above to generate SNPs and invariant sites. We retained only sites where 10 of 13 samples
190 (~80%) had called genotypes, resulting in 3,778,609 SNPs and 26,939,196 invariant sites.

191 Finally, to make a 'synonymous sites' dataset, we started with the '80% called' dataset
192 and used the *M. aurantiacus* gene annotation to select only sites in the 3rd codon position of
193 coding sequences that were four-fold degenerate, i.e., any nucleotide change to that site in the
194 reference background would not change the protein sequence, using a custom script by Tim
195 Sackton (Sackton, 2014/2022). The 'synonymous sites' dataset included 967,470 SNPs and
196 1,654,798 invariant sites. We note that multiple mutation hits within a single codon are
197 possible given our large divergence times, and could change the synonymous nature of these
198 sites, but we don't expect these events to affect our overall results.

199

200 *Phylogenetic tree building*

201 To determine phylogenetic relationships among our samples, we built a maximum
202 likelihood phylogenetic tree using the GTR+Gamma model in RAxML v8.2.12 (Stamatakis, 2014)
203 with SNPs from the '80% called' dataset. SNPs were extracted into a concatenated fasta
204 alignment using the 'consensus' function from bcftools v1.13 (Danecek et al., 2021) and
205 invariant sites were excluded. Heterozygous sites were initially coded as IUPAC ambiguity
206 codes, then randomly converted to a single allele with the 'randbase' function in seqtk v1.3 (Li,
207 2018). We ran 10 separate iterations of RAxML with unique random seeds, then chose the
208 iteration with the largest log-likelihood. We used the RAxML -b option to run 1000 rapid
209 bootstrap trees. We also generated a neighbor-joining tree with 1000 bootstrap replicates from
210 the same data, using the dist.ml, nj, and boostrap.phyDat functions in the R package phangorn
211 (Schliep, 2011).

212 We generated gene trees to examine patterns of gene tree discordance on the
213 phylogeny. We used SNPs from the 'filtered' dataset for each of the 22,421 genes in the *M.*
214 *aurantiacus* genome annotation, following the same approach as above to generate a
215 maximum-likelihood phylogenetic tree in RAxML for each gene. Genes with insufficient data to
216 resolve a tree (any individual with no called sites, or any two individuals with identical
217 sequence) were excluded, resulting in trees for 17,573 genes. We then input these trees into
218 ASTRAL v5.6.1 (Rabiee et al., 2019) which uses a multispecies coalescent approach to calculate
219 a consensus species tree and quartet support scores for each node.

220

221 *Quantifying homozygosity, diversity, and divergence*

222 Pairwise sequence differences were calculated from the 'synonymous sites' dataset using
223 the 'dxy' and 'pi' functions in the program pixy v1.2.3 (Korunes & Samuk, 2021). For each
224 comparison, sequence differences were calculated in 1Mb windows across the genome, then
225 added together and divided by the total number of informative sites. We calculated pairwise
226 diversity (π_s) for each pair of individuals within a species, pairwise divergence (d_s) for each pair
227 of individuals across species, and heterozygosity (h_s, pairwise diversity within an individual) for
228 each individual. Diversity, divergence, and heterozygosity values were averaged across each
229 species or species pair.

230 To estimate the divergence times between species, we used the following molecular
231 clock formula: (divergence time in generations) = (synonymous divergence – synonymous
232 ancestral diversity)/(2*mutation rate). We assumed ancestral diversity for any two species to
233 be the average of within-species diversity for the two species, and took the mutation rate to be
234 1.5x10^-8 (Koch et al., 2000). These estimates are approximate, as they do not take into
235 account the effect of changing effective population sizes, such as demographic bottlenecks, or
236 the possibility that ancestral diversity was very different from current diversity.

237

238 *Quantifying introgression*

239 To explore historical introgression between species, we used three complementary
240 approaches: ABBA-BABA tests and the related *f*-statistics; gene tree discordance bias using
241 TWISST; and the model-based TreeMix program.

242 We used Dsuite v0.4 (Malinsky et al., 2021) to calculate Patterson's D, a measure of the
243 relative frequency of ABBA and BABA sites in the genome, and the related *f4* statistic, which
244 uses allele frequencies to estimate the proportion of the genome resulting from introgression.
245 We calculated D and *f4* for all possible trios of species in our dataset, using both the
246 'downsampled' and '80% called' SNP datasets, with the *M. aurantiacus* complex as the
247 outgroup. Z-scores and associated p-values were calculated for each trio using a block-jackknife
248 approach with 100 blocks in Dsuite; to account for multiple tests, a Bonferroni correction was
249 used to obtain a corrected p-value (p_{corr}). Because there are multiple trios available to estimate
250 introgression for the same pair of species, we summarized results across trios using the F_{branch}
251 statistic in Dsuite for each species pair (Malinsky *et al.* 2018).
252 We used TWISST (github version d56cefb) (Martin & Van Belleghem, 2017) to obtain the
253 proportion of gene trees supporting particular tree topologies. For each trio of species, we
254 compared the two possible alternate (different from the consensus specie tree) tree topologies
255 using a binomial test with expected ratio 1:1 to look for an excess of one topology over
256 another. The *M. aurantiacus* complex was always used as the outgroup. This test is analogous
257 to the SNP-based ABBA-BABA test, but uses gene trees rather than SNPs.
258 We used TreeMix (Pickrell & Pritchard, 2012) to create phylogenetic network models
259 with or without migration edges as a further test of introgression. We used the 'synonymous
260 sites' dataset, including only variant SNPs with no missing data, and grouped individuals by
261 species. The dataset was pruned to select SNPs not in linkage disequilibrium using a custom
262 script by Joana Meier (https://github.com/joanam/scripts/raw/master/ldPruning.sh). We ran

263 models with zero to four migration edges, with 10 replicate runs per model type. The program
264 OptM (Fitak, 2021) was used to define the best fitting TreeMix migration model.
265
266 *Identifying candidate windows with historical introgression*
267 To identify candidate genomic regions with signatures of historical introgression, we
268 used Dsuite (Malinsky et al., 2021) to calculate the window-based *df* statistic (Pfeifer and
269 Kapan, 2019) for windows of 100 informative SNPs, each overlapping the previous by 50 SNPs.
270 We calculated *df* across the genome for three focal trios with strong support for introgression,
271 using the *M. aurantiacus* complex as the outgroup. In each quartet, we selected the 100
272 windows (out of 9594 to 17530, depending on the quartet) with the most extreme (positive or
273 negative) values as potential candidates of introgression, with positive values set to match the
274 direction of the genome-wide F_{branch} signal.
275
276 *Measuring reproductive barriers*
277 We assessed three different barriers to reproduction: postmating prezygotic isolation,
278 F1 hybrid seed inviability, and F1 hybrid sterility. We conducted hand pollinations of
279 greenhouse-grown plants within and among species by first removing anthers from the
280 maternal flower to prevent self-pollination, then using forceps to place pollen from the paternal
281 flower on the maternal stigma surface. Stigma lobes in these species close quickly in response
282 to touch, so hand-pollination is not always successful. In a few cases, supplemental pollen from
283 the same paternal plant was added the following day once the stigma had re-opened. We
284 collected mature, browned fruits, categorized according to cross type. Cross type throughout

285 this paper refers to the combination of maternal species and paternal species, with maternal
286 species always listed first; the 16 cross types are JxJ, JxB, BxJ, JxF, FxJ, JxS, SxJ, BxB, BxF, FxB,
287 BxS, SxB, FxF, FxS, SxF, SxS where J=*M. johnstonii*, B=*M. brevipes,* F=*M. fremontii*, S=Sespe creek
288 population. For the cross type BxF, we also germinated and grew F1 hybrids from four
289 independent crosses in the same conditions as parental plants (Table S3). These F1 hybrids
290 were crossed to themselves and reciprocally with *M. fremontii* and *M. brevipes* as above (cross
291 types HxB, BxH, HxH, HxF, FxH, where H=F1 hybrid).

292 To measure postmating prezygotic isolation, we quantified crossing success (probability
293 that a pollination produces at least one seed) and seed production (number of seeds per fruit)
294 after hand-pollination. To test for an association between cross type and crossing success, we
295 ran a penalized Firth regression with a binomial family function using the R package 'brglm'. A
296 Firth regression was chosen to account for complete separation (all successes or all failures) of
297 some groups. To further test the dominance relationships of this barrier, we compared the
298 crossing success of *M. brevipes* x *M. fremontii* F1 hybrids to their parental species. we ran a
299 generalized linear mixed-effects model (GLMM) with a binomial family and logit link function
300 using the R package 'lme4' on cross types BxB, BxH, BxF, HxB, HxH, HxF, FxB, FxH, and FxF,
301 where H indicates F1 hybrid offspring from a BxF cross. For this model, maternal population
302 was included as a random effect, treating each independent F1 cross as its own population.

303 To assess seed viability in each cross, we used a combination of visual inspection and
304 chemical treatment. All seeds were inspected under a dissecting scope and scored as inviable or
305 viable. Viable seeds were plump and generally ovate, although they were allowed to be slightly
306 misshapen as long as they appeared to be full. Inviable seeds included any seed that was

307 severely shriveled, concave, empty, much smaller than the typical within-species seed, or with a
308 shape very different from the typical ovate shape. To confirm that seeds visually scored as
309 inviable were in fact inviable, we treated a subset of seeds with tetrazolium chloride, which
310 stains viable seeds dark red. For this treatment, seeds were scarified using 1:5 bleach:distilled
311 water with 0.83 uL/mL Triton-X for 15 minutes, washed twice with distilled water, and placed in
312 1% (w/v) tetrazolium chloride, then incubated in the dark at room temperature for ~48 hours.
313 To test for an association between cross type and the relative counts of viable vs. inviable
314 seeds, we ran a penalized Firth regression using the R package 'brglm' with a binomial family
315 and logit link function. A Firth regression was chosen to account for complete separation (all
316 viable or all inviable) of some groups.

317 To investigate reciprocal differences in seed size, a predicted correlate of parental
318 conflict-driven hybrid seed inviability (Haig & Westoby, 1991), we imaged a subset of seeds
319 from 49 fruits under a dissecting scope and used imageJ to manually measure seed length and
320 width. We ran a linear mixed-effects model using the R package 'lme4' to test for differences in
321 seed length between the four intraspecific cross types (JxJ, BxB, FxF, and SxS), using fruit as a
322 random effect. We also ran six independent LMMs, one for each pair of species, to directly
323 compare intra- and interspecific seeds. For example, we tested the *M. johnstonii* vs. *M. brevipes*
324 pair by comparing cross types JxJ, JxB, BxJ, BxB. For each species-pair, we ran one LMM to test
325 for an association between cross type and seed length, and a second to test for an association
326 between cross type and seed length/width ratio.

327 To assess hybrid male sterility, we scored pollen number and pollen viability using an
328 aniline blue stain. For each individual, all anthers from a single flower were collected in 50 µL

329 0.25% aniline blue in lactophenol solution. Blue stained pollen grains were scored as viable,
330 while unstained clear pollen grains were counted as inviable. Pollen was counted in full $1mm^2$
331 squares of a hemocytometer until 9 squares or at least 100 total pollen grains were counted.
332 For each individual, we estimated pollen viability by determining the proportion of viable pollen
333 grains out of the total counted (for some individuals, pollen viability was measured from
334 multiple flowers and the average was used). We used an LMM to test for an association
335 between species ID and the total count of pollen grains scored per hemocytometer square, with
336 population as a random effect. Similarly, we used a GLM with a binomial family and logit link
337 function to test for an association between species ID (*M. brevipes, M. fremontii,* or F1 hybrid)
338 and the relative counts of viable vs. inviable pollen grains, adding population as a random effect
339 (each hybrid family was treated as its own population).

340 To assess *M. brevipes-M. fremontii* F1 female fertility, we hand-pollinated F1 hybrids
341 with pollen from either parent and measured seed production. To determine whether F1
342 hybrids produce fewer seeds than within-species crosses, we used a linear model to test for an
343 association between cross type and the number of seeds produced per fruit, comparing cross
344 types BxB, BxH, HxF, and FxF and only counting fruits that produced at least one seed. Maternal
345 population was included as a random effect and each F1 hybrid family was treated as a
346 separate population.

347 For every statistical model above, we ran Tukey post-hoc tests implemented in the
348 package 'multcomp' to test for pairwise differences between each cross type or group.

349 We followed the methods of Sobel and Chen (2014) to calculate standardized measures
350 of reproductive isolation for each of three reproductive barriers, as well as total postmating
351 reproductive isolation. All measures used the equation

352 $$RI = 1 - 2 * (H/(H + C))$$

353 where H=heterospecific fitness and C=conspecific fitness. In this framework, RI ranges from -1
354 to 1 where -1 is complete heterosis, 0 is random assortment, and 1 is complete isolation. We
355 calculated total measured reproductive isolation sequentially with the equation

356 $$RI_{TOTAL} = RI_{previous} + \left(1 - RI_{previous}\right) * RI_{new}$$

357 where $RI_{previous}$ is the total RI from all previous barriers and RI_{new} is the next barrier. Barriers that
358 could not be measured due to complete or near-complete previous RI were left blank.
359

360 **RESULTS**

361 **Genome-wide variation in the *M. brevipes* group defines clear species but also reveals a**
362 **complex history of introgression.**

363 A maximum-likelihood phylogeny generated from whole-genome SNP data resolves each
364 of the three focal species (*M. brevipes*, *M. johnstonii*, and *M. fremontii*) as monophyletic with
365 100% bootstrap support (Figure 1C). Within these species, each population is also recovered as
366 monophyletic, with the exception of one sample from a *M. brevipes* population (Figure 1C: one
367 individual from population B11 clusters with B19). *M. johnstonii* is supported as sister to *M.*
368 *brevipes,* in contrast to (Beardsley et al., 2004) which found *M. brevipes* and *M. fremontii* as
369 sister based on just three loci. Genome-wide estimates of pairwise nucleotide divergence at
370 synonymous sites also support strong divergence among the three focal species, with pairwise

371 divergence values (d_s, 4.8-6.0%) consistently well outside the range of nucleotide diversity
372 within species (π_s, range 1.6-3.7%) (Figure 1D, Table S4). Heterozygosity is similar to pairwise
373 diversity (h_s, range 1.1-3.1%), supporting a primarily outcrossing strategy in these species.
374 Speciation times were estimated at >1 million generations for all species pairs (Figure 1C).
375 The Sespe Creek population (S25) is clearly a distinct lineage well outside of the *M.*
376 *brevipes* trio. Although S25 is most closely related to *M. constrictus*, high genetic divergence
377 between these lineages (d_s = 0.06) suggest they are distinct species (Figure 1D, Table S4). Other
378 species in this clade are not sampled and could be closer relatives to Sespe Creek, but none are
379 known to occur in that geographic area. *M. nanus* is recovered as an outgroup to the other
380 *Eunanus* section species as expected, with the *M. aurantiacus* complex set as the ultimate
381 outgroup (Figure 1C).

382 Despite clear divergence between among these *Mimulus* species, we also discovered
383 substantial historical introgression. Using ABBA-BABA tests (Table 1, Table S5) and associated *F*
384 statistics (Figures 2A and S2), TWISST (Figure S3), and TreeMix (Figure S4), we detected three
385 signals of gene flow that were consistent across all methods. The first of these signals supports
386 directional introgression from the *M. brevipes-M. fremontii-M. johnstonii* clade into the Sespe
387 Creek population (Table 1: *D* = 0.135-0.149; Figure 2A: F_{branch} = 4.8-5.9%, Figure S3: TWISST
388 quartets 41.1/41.8/17.0, Figure S4: TreeMix m=0.193). A second, weaker signal of introgression
389 occurs in the reciprocal direction from the *M. constrictus*-Sespe Creek clade into the *M.*
390 *brevipes-M. fremontii-M. johnstonii* clade (Table 1: *D* = 0.027-0.046, Figure 2A: F_{branch} = 0.4-
391 1.3%, Figure S3: TWISST quartets 70.3/15.7/14.0, Figure S4: TreeMix m=0.021). Finally, a third
392 signal of introgression was detected between *M. nanus* and the clade containing *M. constrictus*

393 and Sespe Creek (Table 1: D = 0.101-0.178, Figure 2A: F_{branch} = 2.4-3.4%, Figure S3: TWISST
394 quartets 73.5/15.2/11.3, Figure S4: TreeMix m=0.296). We summarize these patterns in Figure
395 S5, but note that shared evolutionary history makes it challenging to assign introgression events
396 to single lineages.

397 For each of these three general cases, we chose the trio with the strongest signal and
398 scanned the genome for signatures of introgression using the statistic *df*. Outlier *df* windows
399 were asymmetric, with more positive outliers (signals of introgression consistent with the
400 genome-wide F_{branch} pattern) than negative outliers of the same magnitude (Figure 2B). Positive
401 outliers were widely distributed throughout the genome, present on all ten linkage groups for
402 all three trios and with no large blocks of uninterrupted introgression, indicating that gene flow
403 in this group is ancient rather than ongoing.

404

405 **Multiple strong postmating reproductive barriers between species in the *M. brevipes* group.**

406 Most crosses between four focal species (*M. johnstonii, M. brevipes, M. fremontii,* and
407 the Sespe Creek population) showed little to no reduction in crossing success (probability of
408 producing a seed, or seeds produced per fruit) compared to within-species crosses (Figures 3
409 and S6, Table S6). In one case (FxB), there is evidence of unidirectional postmating prezygotic
410 isolation: only one in 58 crosses between maternal *M. fremontii* and paternal *M. brevipes*
411 produced any seeds, a significantly lower proportion than the within-species or reciprocal cross
412 types (Figure 3, Table S6). This pattern appears to be additive on both the maternal and
413 paternal sides in *M. brevipes* x *M. fremontii* F1 hybrids, with intermediate crossing success in
414 both HxB and FxH crosses (Figure S7). A few other interspecific cross types also had low or zero

415 seed production (e.g., reciprocal crosses of *M. fremontii* and Sespe Creek), which could indicate
416 a postmating prezygotic barrier, but these crosses had low sample sizes and did not reach
417 significance compared to within-species crosses.

418 For crosses that did produce seeds, we found strong F1 hybrid seed inviability (viability
419 <2%) in nine interspecific crosses (Figure 4A-B, Table S6). The exception was species pair *M.*
420 *fremontii* and *M. brevipes,* which produced viable seeds in both directions (Figure 4A-B, Table
421 S6). We could not score seed viability for cross type SxF because the only potential seeds
422 produced were not distinguishable from unfertilized ovules.

423 *M. johnstonii* intraspecific seeds were significantly larger than *M. brevipes* or *M.*
424 *fremontii* seeds, with Sespe Creek seeds intermediate in size (Figure 4C). Inviable seeds overall
425 showed no evidence of overgrowth or undergrowth relative to parents, but instead tended to
426 match the seed length of the maternal parent. However, F1 hybrids with Sespe Creek as
427 maternal parent did have slightly smaller seeds than either parent (this trend was only
428 significant for SxF) (Figures 4A and S8A). Crosses with *M. johnstonii*, the largest-seeded species,
429 as the maternal parent produced inviable seeds that were collapsed and thin, as shown by a
430 significant increase in hybrid seed length/width ratios (three cross types) compared to both
431 parents and to the reciprocal cross type (Figures 4A and S8B). In the reciprocal direction, hybrid
432 seeds were typically shriveled, as were hybrid seeds in both directions of Sespe Creek crosses.
433 (Figures 4A and S8B).

434 Although in most cases, strong seed inviability prevented us from quantifying later-
435 acting barriers, we were able to assess F1 hybrid sterility between *M. brevipes* and *M.*
436 *fremontii*. Pollen number per flower was intermediate for hybrids compared to the two

437 parental species (Figure 5A). However, only ~20% of hybrid pollen grains were fertile, a sharp
438 reduction from either parent, indicating strong F1 male sterility (Figure 5B). We find no
439 evidence of hybrid female sterility in *M. brevipes* x *M. fremontii* F1s; seed production from
440 pollinated hybrids was intermediate compared to pure species (Figure 5C).

441 Total postmating reproductive isolation was near-complete (RI>=0.95) for all tested
442 species pairs except for *M. brevipes* vs. *M. fremontii,* primarily driven by strong hybrid seed
443 inviability (Table 2). The exception, *M. brevipes* vs. *M. fremontii,* had incomplete but still
444 substantial total postmating RI from a combination of postmating prezygotic isolation and F1
445 male sterility (B > F: RI=0.91; F > B: RI=0.66).

446

447 **DISCUSSION**

448 A major goal of speciation research is to understand similarities and differences in how
449 reproductive isolation emerges as groups of species diverge. We find that *Mimulus brevipes,*
450 *Mimulus johnstonii, and Mimulus fremontii* are clearly delineated species both genetically and
451 by intrinsic reproductive barriers. We find strong hybrid seed inviability between multiple
452 species pairs, as well as a postmating prezygotic barrier and severe hybrid male sterility
453 between one species pair. While premating barriers have not yet been thoroughly quantified in
454 this group, the combination of close geographic proximity (within centimeters in some cases)
455 and similar floral morphology (excluding *M. brevipes*) makes it unlikely that premating barriers
456 alone can eliminate hybridization. These strong postmating barriers are therefore likely
457 important in preventing contemporary gene flow.

While many studies have shown that reproductive isolation increases with divergence on average, individual species pairs are often idiosyncratic (Coyne & Orr, 1989; Malone & Fontenot, 2008; Matute & Cooper, 2021; Moyle et al., 2004). Our results highlight this heterogeneity – while reproductive isolation and divergence are both strong overall, the species pair with the least postmating reproductive isolation in this group (*M. brevipes* and *M. fremontii*) is not the most recently diverged pair (*M. brevipes* and *M. johnstonii*). Paying greater attention to the exceptions may help us better understand the factors that drive reproductive isolation.

Gene discordance and introgression

We find evidence of extensive phylogenetic discordance across the genome, including signatures of historical introgression between multiple species in this group. These signals are scattered throughout the genome and broken up by generations of recombination; we find no evidence of recent or ongoing introgression. Without further sampling of populations and species in this section, attributing these signals to precise events on the phylogeny is difficult. Taken as a whole, however, they demonstrate a high degree of complexity in the divergence process, consistent with reticulate evolutionary histories of other groups within *Mimulus* (e.g., Brandvain et al., 2014; Nelson et al., 2021; Stankowski et al., 2019), in plants more broadly (e.g., Curtu et al., 2009; Goulet et al., 2017; Hamlin et al., 2020; Kay et al., 2018; Scascitelli et al., 2010), and across the tree of life (e.g., D'Angiolo et al., 2020; Green et al., 2010; Kleindorfer et al., 2014; Mallet et al., 2007; Schumer et al., 2018). Without postmating reproductive barriers, even small amounts of introgression can lead to species collapse in sympatry, especially if premating barriers are disrupted by environmental change (Behm et al., 2010; Kleindorfer et

480 al., 2014; Xiong & Mallet, 2022). Alternatively, species can persist despite ongoing
481 introgression, depending on the circumstances (Kay et al., 2018; Kenney & Sweigart, 2016;
482 Servedio & Hermisson, 2020). Past introgression in the *Eunanus* group may have predated the
483 evolution of the strong postmating barriers we see today. We argue that postmating
484 reproductive barriers likely played an important role in reducing gene flow as divergence
485 increased.

486 *Cryptic diversity in Mimulus section Eunanus*

487 Genetic data allow us to uncover cryptic variation in the form of distinct genetic lineages
488 that are not readily distinguished by morphological features in the field (Bickford et al., 2007;
489 Struck et al., 2018). Our population from Sespe Creek does not appear to match any of the
490 likely species from the area, and we find that it is a genetically distinct lineage with a history of
491 introgression. In addition, it appears to be reproductively isolated from other members of the
492 group by strong hybrid seed inviability. We do not yet know the exact nature of its origin, or
493 how widely distributed this lineage is; more sampling from the area and genetic data from
494 more species in the group will be necessary to fully resolve these questions. Studies of
495 speciation in plants often focus on ecologically mediated premating reproductive isolation, but
496 cryptic diversity may be better explained by postmating barriers (Coughlan & Matute, 2020).
497 *Mimulus* section *Eunanus* is home to many more understudied, small, pink-flowered taxa; if our
498 study is any indication, strong postmating reproductive isolation may play an outsized role in
499 generating diversity in this group.

500 *Parallel evolution of hybrid seed inviability in Mimulus*

501 Hybrid seed inviability has been found repeatedly in species pairs from the *Mimulus*
502 *guttatus* species complex (section *Simiolus*) (Coughlan et al., 2020; Oneal et al., 2016; Sandstedt
503 & Sweigart, 2022). By demonstrating hybrid seed inviability in a distant section of *Mimulus,* we
504 show that this pattern is widespread and important, both across *Mimulus* and likely in plants
505 more broadly. In the *M. guttatus* complex and other systems, hybrid seed inviability has been
506 tied to parental conflict in resource allocation, a process mediated by the endosperm (Coughlan
507 et al., 2020; Haig & Westoby, 1991; Lafon-Placette et al., 2017; Oneal et al., 2016; Rebernig et
508 al., 2015; Roth et al., 2019; Sandstedt & Sweigart, 2022). We do not find clear evidence of
509 parental conflict in our system -- hybrid seed sizes tended to track maternal seed sizes, without
510 the telltale overgrowth or undergrowth phenotypes. However, hybrid seed size is not always a
511 good predictor of parental conflict (Sandstedt & Sweigart, 2022), so future work to characterize
512 differences in seed development would be required to rule out a conflict hypothesis.
513 Alternatively, differences in parental seed sizes between our species could result in
514 Dobhzansky-Muller-like incompatibilities during hybrid seed development, without invoking
515 parental conflict as a driver. Seed size is an important life history trait tied to ecological
516 strategies; larger seeds tend to have more success establishing under a variety of hazardous
517 conditions, from nutrient deprivation to low soil moisture to deep burial (Leishman et al.,
518 2000). Larger, heavier seeds may also prevent long-range dispersal and keep offspring in
519 maternal habitats for which they are locally adapted, as is the case in dune-adapted plants
520 (Bowers, 1982; Schwarzbach et al., 2001). Both *M. johnstonii* and the Sespe Creek population
521 are found on unstable scree slopes, which may pose a particular challenge to seed
522 establishment or favor local dispersal to maintain local adaptation. This habitat preference is

523 therefore a possible candidate for a selective force, which could have acted in parallel in *M.*
524 *johnstonii* and Sespe Creek to drive seed size differences leading to hybrid inviability.
525 *Postmating prezygotic isolation*
526 Crossing failure (postmating prezygotic isolation) can be caused by a failure of pollen
527 tube germination, failure of pollen tube growth, failure of fertilization, or even early seed
528 abortion (Wheeler et al., 2001); it may be a passive incompatibility between pollen and pistil, or
529 an active rejection mechanism to prevent maladaptive hybridization (Hogenboom et al., 1975;
530 Roda & Hopkins, 2019; Rushworth et al., 2022). Most studies on the mechanisms of postmating
531 prezygotic isolation come from systems with self-incompatibility, where they are thought to be
532 related to self-incompatibility mechanisms, e.g. *Solanum* (Bernacchi & Tanksley, 1997; Tovar-
533 Méndez et al., 2014), *Nicotiana* (Kuboyama et al., 1994), and *Lilium* (Ascher & Drewlow, 1975),
534 though a mechanism unrelated to self-incompatibility has been described in *Brassica* (Fujii et
535 al., 2019). Since *Mimulus* lacks self-incompatibility mechanisms, this group provides an
536 opportunity to investigate how interspecific incompatibility may arise on its own. In other
537 systems with differences in style length, germinating pollen tubes can under- or over-shoot the
538 ovules (Gore et al., 1990; Williams & Rouse, 1988). Style length could be important in our
539 system, since *M. brevipes* styles are substantially longer than *M. fremontii* styles, though our
540 case is unusual in that pollen from the long-styled parent fails while pollen from the short-
541 styled parent is successful. Pollen competition driving differential coevolution of the pollen and
542 pistil is another possible source of incompatibilities (Brandvain & Haig, 2005; Skogsmyr &
543 Lankinen, 2002), a scenario which has been documented in the *M. guttatus* complex (Aagaard
544 et al., 2013; Fishman et al., 2008) and *Arabidopsis* (Takeuchi & Higashiyama, 2012).

545 *Hybrid male sterility*

546 Hybrid male sterility has been characterized multiple times in *Mimulus* sections Simiolus
547 and Erythranthe, with a variety of genetic causes, including a nuclear DMI interaction (Sweigart
548 et al., 2006), a cytoplasmic-nuclear interaction (Fishman & Willis, 2006), or underdominant
549 chromosomal rearrangements (Stathos & Fishman, 2014), but the relative frequency of these
550 mechanisms across plants is unknown. *M. brevipes* and *M. fremontii* are more genetically
551 divergent than most pairs for which male sterility has been studied, in *Mimulus* or elsewhere.
552 Since they still produce viable hybrids and sterility is not 100% complete, genetic mapping could
553 be used in the future to determine the mechanisms underlying sterility in this system, and the
554 degree of parallelism with other cases in *Mimulus.*

555 *Future directions*

556 As the first in-depth genomic and phenotypic investigation of speciation within *Mimulus*
557 section *Eunanus,* this study demonstrates the utility of understudied or overlooked species
558 groups for enriching our understanding of the speciation process. We find evidence that hybrid
559 seed inviability and hybrid male sterility are important barriers across disparate groups in
560 *Mimulus,* and may be underappreciated in plants more generally. Key features of this system
561 provide fruitful avenues for future mechanistic study: seed size evolution and hybrid seed
562 inviability; style length and postmating prezygotic isolation; and highly divergent hybrid male
563 sterility are all worthy of future exploration. This study also provides a starting point for a more
564 complete phylogenetic sampling of section *Eunanus*, which would enhance our understanding
565 of cryptic divergence and the interplay between ecological, geographic, and genetic forces
566 driving the diversification of species.

567 **Author contributions**

568 Research conceived and designed jointly by M.C.F and A.L.S. Data collected and analyzed by

569 M.C.F. Manuscript written by M.C.F and A.L.S.

570 **Data accessibility**

571 All whole genome sequence data will be deposited at the NCBI Sequence Read Archive upon

572 acceptance of this publication. Other data will be made available on Dryad Digital Repository.

573 **Acknowledgments**

574 We thank James Sobel for seed collections, for advice on germination and growth conditions,

575 and for helpful discussions. Samuel Mantel, Makenzie Whitener, Natalie Gonzalez, and Emma

576 Chandler provided comments that improved the manuscript. Kelly Dyer, Jill Anderson, Casey

577 Bergman, Molly Schumer, John Willis, Jenn Coughlan, Elen Oneal, and Robert Franks also

578 contributed to useful discussions. This work is supported by the National Science Foundation

579 (award 1856180); the National Institutes of Health Predoctoral Training Grant (award

580 5T32GM007103), the Society for the Study of Evolution Lewontin Award, and a UGA Plant

581 Center Doctoral Dissertation Improvement Grant.

582 The authors declare no competing interests.

583

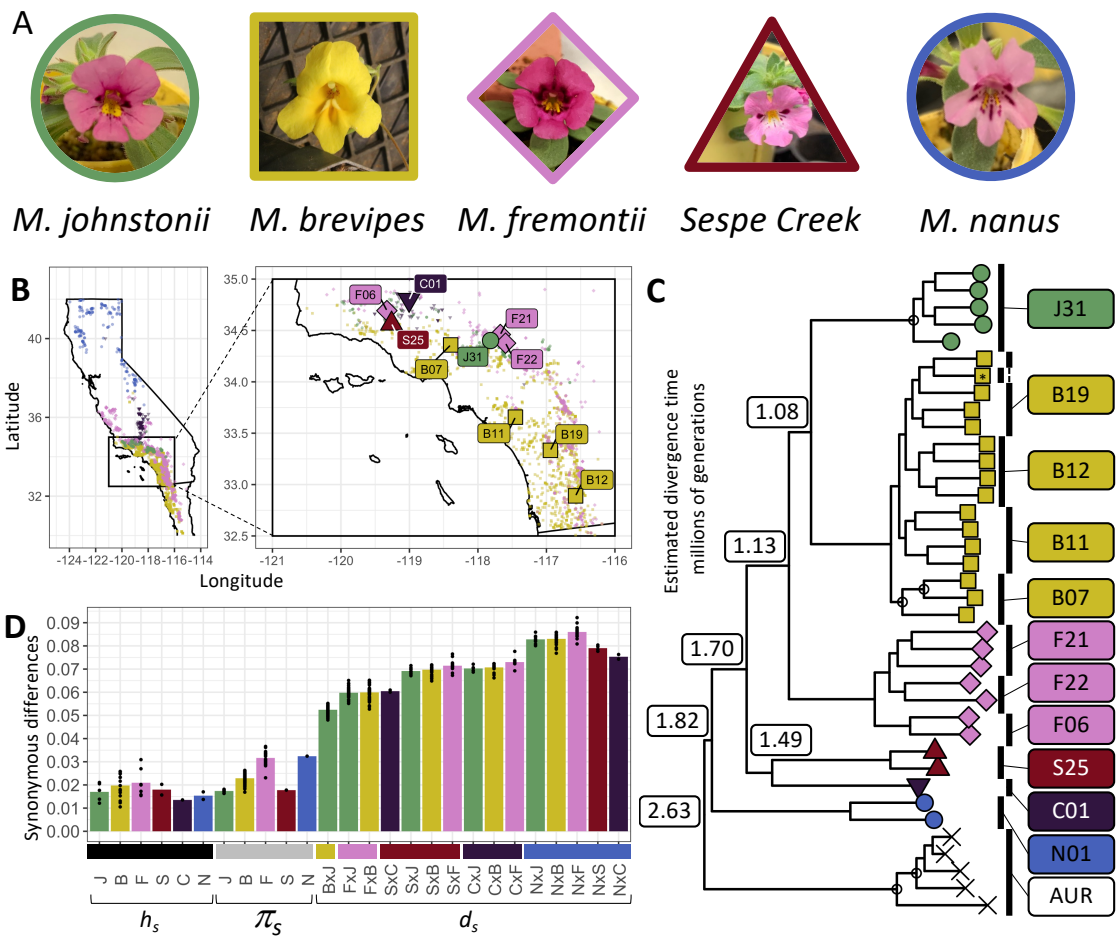

Figure 1. Phylogenetic relationships and divergence between sampled species in *Mimulus* section *Eunanus*. (A) Representative floral images for sampled species. (B) Map of occurrence records and sampled populations from the GBIF database for five species within California and Baja California. Inset highlights focal region for sampling, where species ranges overlap. Smaller icons indicate GBIF records for each species, which include iNaturalist research grade observations and herbarium collections. Larger named icons indicate sampled populations used in this study. The range of *M. nanus* extends into Nevada, Oregon, and Washington; population N01 (*M. nanus*) was collected from Washington state and is not shown. Population S25, referred to as Sespe Creek, is treated as a separate lineage. (C) Maximum likelihood phylogeny inferred using RAxML from the '80% called' dataset of genome-wide SNPs, rooted by the *M. aurantiacus* complex. All nodes except those marked with open circles have 100% bootstrap support. Species divergence times were estimated using synonymous divergence relative to synonymous diversity. All sampled populations are monophyletic with strong support, with the exception of one sample from B11 that clusters with B19 (marked with an asterisk). (D) Nucleotide heterozygosity (h_s), pairwise diversity (π_s), and divergence (d_s) at genome-wide synonymous sites, indicating substantially higher between-species divergence than within-species diversity. Bars represent species or comparison means, while points represent

individual pairwise sample comparisons. Diversity includes both within- and between-population comparison where possible. Sespe creek is substantially diverged from its closest sampled relative, *M. constrictus* (SxC d_s=6.0%). J = *M. johnstonii*, B = *M. brevipes,* F = *M. fremontii*, S = Sespe creek population, C = *M. constrictus*, N = *M. nanus*, AUR = *M. aurantiacus* complex.

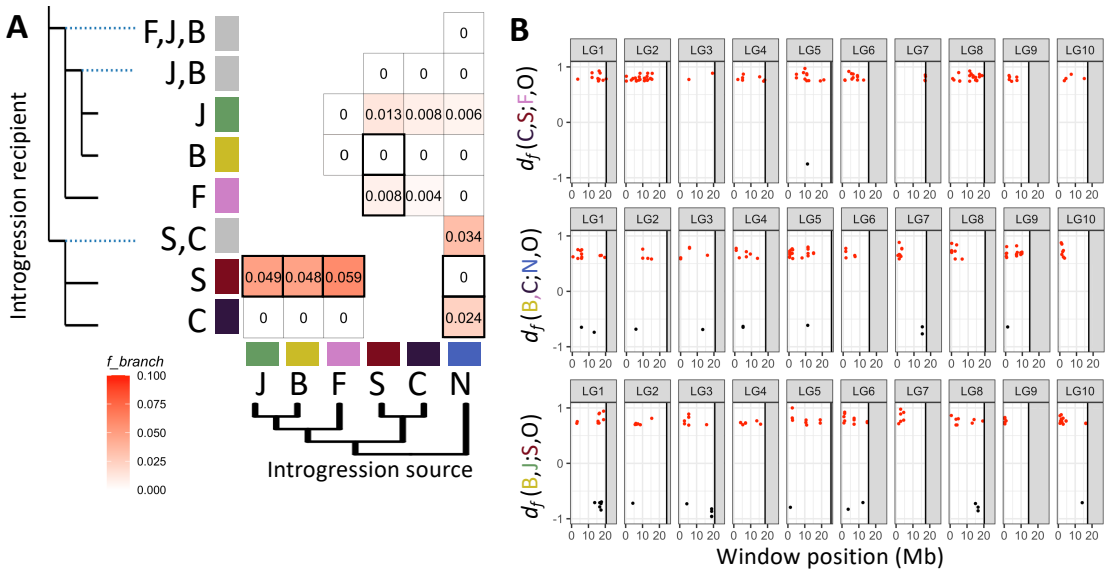

Figure 2. Signatures of historical introgression between species in *Mimulus* section *Eunanus*. (A) Genome-wide F_{branch} statistics, an estimate of the proportion of the genome affected by introgression based on correlated *f4* statistics, using the downsampled SNP dataset. All listed nonzero F_{branch} values are supported by ABBA-BABA tests with Bonferroni-corrected p-value < 0.001. Seven bold-outlined boxes indicate comparisons with significant gene discordance bias supporting introgression from TWISST gene tree summaries, using Bonferroni-corrected p-values <0.01. Full TWISST summaries are in Figure S3. (B) Position along ten linkage groups of extreme *df* values in 100-SNP windows for each of three tested quartets. Each quartet (P1,P2;P3,O) tests for signatures of introgression from P3 into P2 (positive outliers) or P3 into P1 (negative outliers). The top 100 windows with the largest absolute value of *df* are plotted, with positive *df* values in red and negative in black. From top to bottom, positive outliers show a history of introgression from *M. fremontii* into Sespe Creek, from *M. nanus* into *M. constrictus,* and from Sespe Creek into *M. johnstonii*. Total tested windows for each quartet: 9594, 10429, and 14596, respectively.

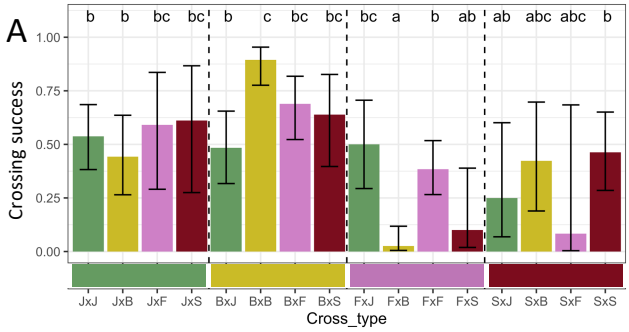

Figure 3. Postmating prezygotic isolation between at least one species pair. Crossing success (probability of producing at least one seed from a cross) for intra- and interspecific cross types. Shown are least-square means and asymptotic confidence intervals from a Firth binomial model. Letters indicate significance in post-hoc Tukey tests; cross types sharing a letter are not significantly different. One interspecific cross type, FxB, was significantly reduced compared to both intraspecific parental crosses, indicating an asymmetric barrier to fruit set. Two other crosses, FxS and SxF, had low fruit set possibly indicating a reproductive barrier, but were not significant in the model due to low sample sizes; e.g., 0 out of 4 SxF crosses resulted in seeds. J = *M. johnstonii*, B = *M. brevipes,* F = *M. fremontii*, S = Sespe creek population.

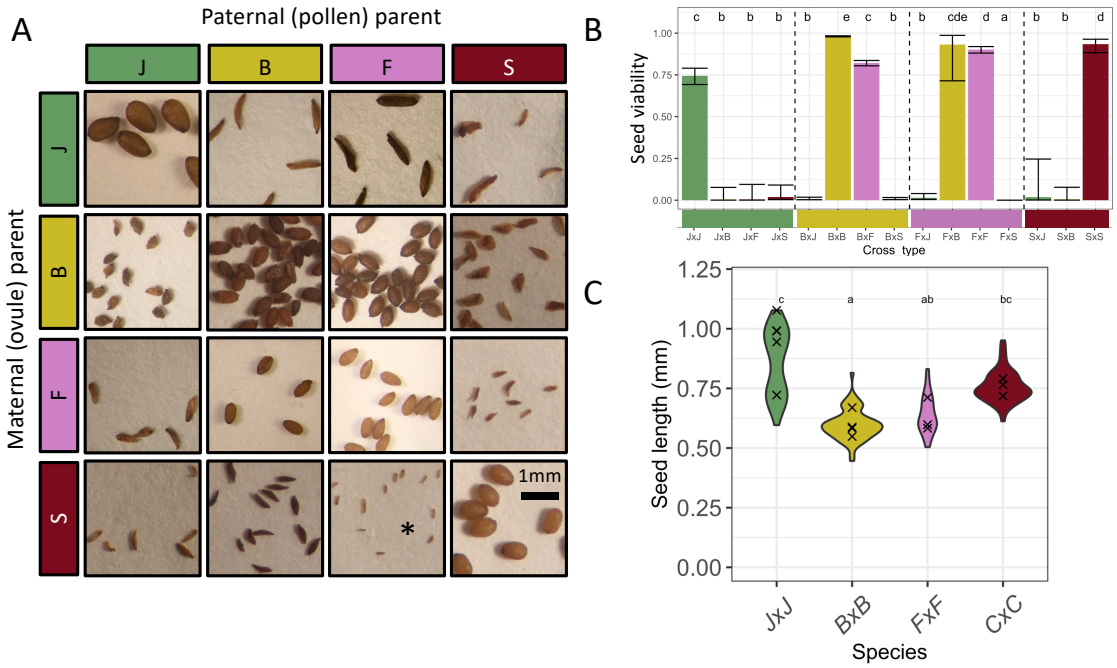

Figure 4. Strong hybrid seed inviability between multiple species pairs. (A) Representative seed images from intra- and interspecific laboratory crosses between four species. All images are adjusted to the same scale. For the SxF cross, marked with an asterisk, the only 'seeds' produced were not distinguishable from unfertilized ovules and were not counted as seeds for

640 crossing success or viability scoring, but it is possible they represent early seed abortion. (B)
641 Proportion of viable seeds produced by intra- and interspecific laboratory crosses. Shown are
642 least-square means and asymptotic confidence intervals from a Firth binomial model, with
643 letters indicating significance in post-hoc Tukey tests. Intraspecific, BxF, and FxB crosses are
644 mostly viable, but all other interspecific cross types have almost complete inviability. (C) Seed
645 lengths for intraspecific crosses. Violin plots show distribution of data for individual seeds, with
646 x's marking the means of individual fruits. Letters indicate significance from post-hoc Tukey
647 tests of an LMM.
648

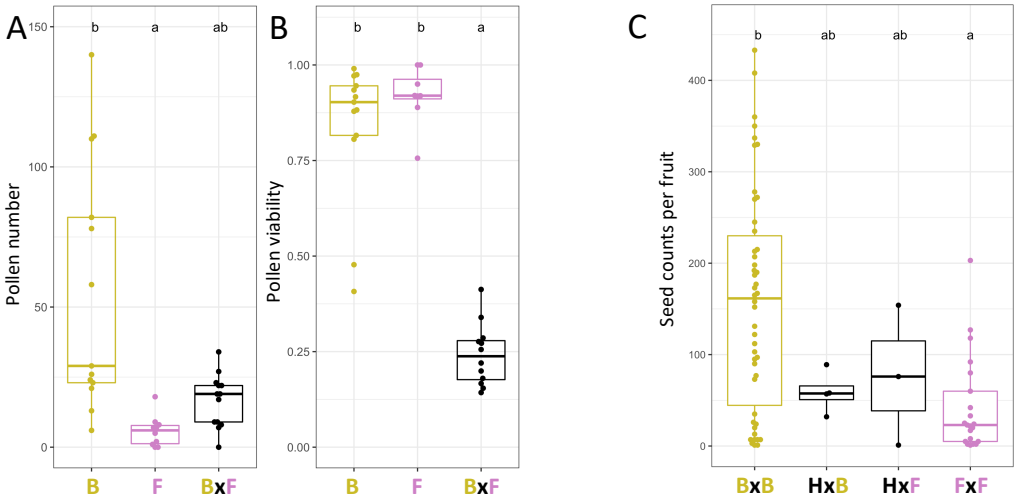

649
650 **Figure 5. Strong hybrid male sterility in hybrids between *M. brevipes* and *M. fremontii*.** (A)
651 Pollen number (counts per mm^2 on a hemocytometer) and (B) pollen viability (proportion of
652 pollen grains scored as viable in aniline blue stain). Letters indicate significance in post-hoc
653 Tukey tests from a poisson (abundance) or binomial (viability) GLMM with population as a
654 random variable. Each point represents the average across 1-3 flowers from a single individual.
655 For each panel, groups sharing a letter are not significantly different. (C) Seed production from
656 hybrid vs. parental fruits as a test of hybrid female sterility, including only fruits that produced
657 at least one seed. Letters indicate significance in post-hoc Tukey tests from a linear model.
658 B=*M. brevipes*, F=*M. fremontii*, H=*M. brevipes x M. fremontii* F1 hybrid.
659
660 **Table 1. ABBA-BABA test results from downsampled SNP dataset**.
661

P1	P2	P3	D	Z-score	Significance	*f4*-ratio	BBAA	ABBA	BABA
J	B	F	0.017	2.8	n.s.	0.009	97294	66664	64434
B	**J**	**S**	0.045	8.0	***	0.013	155429	53359	48765
J	F	S	0.007	1.4	n.s.	0.002	126129	59205	58393
B	**F**	**S**	0.047	9.4	***	0.015	129882	60335	54948
B	**J**	**C**	0.035	6.9	***	0.008	159203	46322	43188

F	J	C	0.005	0.9	n.s.	0.001	131898	51052	50586
B	**F**	**C**	0.027	5.7	***	0.007	135187	51425	48736
C	**S**	**J**	0.142	27.5	***	0.049	103893	69306	52109
C	**S**	**F**	0.149	27.2	***	0.059	103887	70221	52046
C	**S**	**B**	0.135	24.9	***	0.048	106972	68191	52012
B	**J**	**N**	0.031	7.6	***	0.006	215279	41581	39069
F	**J**	**N**	0.030	8.1	***	0.007	185137	46328	43605
F	B	N	0.003	0.8	n.s.	0.001	188742	44743	44481
J	**S**	**N**	0.102	24.3	***	0.028	124410	63335	51623
B	**S**	**N**	0.121	27.3	***	0.034	122382	65553	51390
F	**S**	**N**	0.124	31.0	***	0.034	126189	65090	50688
J	**C**	**N**	0.160	30.7	***	0.049	98813	68692	49743
B	**C**	**N**	0.176	31.9	***	0.055	97995	70669	49509
F	**C**	**N**	0.178	33.7	***	0.055	99391	70192	48945
S	**C**	**N**	0.087	16.9	***	0.024	136174	55129	46312

***p_{corr}<0.001. n.s.=not significant
J = *M. johnstonii*, B = *M. brevipes,* F = *M. fremontii*, S = Sespe creek population,
C = *M. constrictus*, N = *M. nanus*

Table 2. Summary of Postmating Reproductive Isolation (RI).

Pair a, b	Crossing success RI		Seed viability RI		F1 viability RI		**Total measured RI**	
	a>b	b>a	a>b	b>a	a>b	b>a	a>b	b>a
J, B	0.30	0.10	**0.99**	**1.00**	--	--	**0.99**	**1.00**
J, F	-0.13	-0.05	**0.97**	**1.00**	--	--	**0.97**	**1.00**
B, F	**0.91**	0.13	-0.03	0.09	--	**0.57**	**0.91**	**0.66**
J, S	0.35	-0.07	**1.00**	**0.97**	--	--	**1.00**	**0.96**
B, S	0.05	0.16	**1.00**	**0.99**	--	--	**1.00**	**0.99**
F, S	1.00	0.68	--	**1.00**	--	--	1.00	**1.00**

a>b indicates reproductive isolation preventing gene flow from species a into species b, calculated by comparing the fitness of b x a crosses relative to b x b crosses, with b>a indicating the reciprocal direction using the fitness of a x b crosses relative to a x a crosses, following (Sobel & Chen, 2014). **Bolded** values include contributions from barriers with significant model results.

Supplementary Figures and Tables

669

670 **Figure S1. Comparison of phylogenetic methods.** (A) Neighbor-joining tree produced from '80%
671 called' SNP dataset, with heterozygous sites randomly assigned to one allele. (B) Maximum-
672 likelihood tree produced using RAxML from '80% called' SNP dataset using the GTR+Gamma
673 model, with heterozygous sites randomly assigned to one allele. (C) ASTRAL tree produced from
674 17,524 gene trees, each created using RAxML with the GTR+Gamma model using SNPs from the
675 'filtered' SNP dataset within a given gene's coordinates, with heterozygous sites randomly

assigned to one allele. Each node is labelled with the quartet support scores for the consensus, 1st alternative, and 2nd alternative topologies. (D) The same ASTRAL consensus tree shown in (C) but with posterior probabilities for each node.

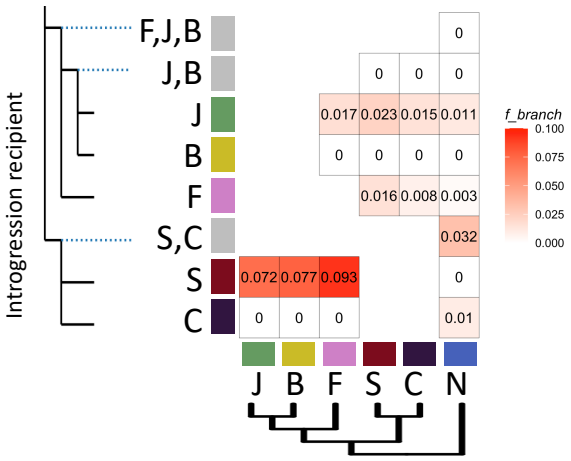

Figure S2. F_{branch} results for full '80% called' SNP dataset. Results are qualitatively consistent with the 'downsampled' dataset (Fig 2) but estimated F_{branch} values tend to be higher for the full dataset. J = *M. johnstonii*, B = *M. brevipes,* F = *M. fremontii*, S = Sespe creek population, C = *M. constrictus*, N = *M. nanus.*

Consensus topology	Alternate topology 1	Alternate topology 2	Binomial Test p_{corr}
C S F O 7207 (41.1%)	F S C O 7330 (41.8%)	F C S O 2987 (17.0%)	<0.001
C S J O 7,253 (41.4%)	J S C O 7,299 (41.6%)	J C S O 2,972 (17.0%)	<0.001
C S B O 7,183 (41.4%)	B S C O 7,287 (41.6%)	B C S O 3,054 (17.0%)	<0.001
F S N O 12,874 (73.5%)	N S F O 2,667 (15.2%)	N F S O 1,983 (11.3%)	<0.001
J S N O 12,869 (73.4%)	N S J O 2,613 (14.9%)	N J S O 2,042 (11.7%)	<0.001
B S N O 12,828 (73.2%)	N S B O 2,638 (15.1%)	N B S O 2,059 (11.7%)	<0.001
C S N O 12,312 (70.3%)	N S C O 2,773 (15.8%)	N C S O 2,439 (13.9%)	<0.001
F C N O 11,114 (63.4%)	N C F O 3,350 (19.1%)	N F C O 3,061 (17.5%)	0.006
B F S O 12,328 (70.3%)	S F B O 2,744 (15.7%)	S B F O 2,452 (14.0%)	0.001
J B F O 8,528 (48.7%)	F B J O 4,673 (26.7%)	F J B O 4,323 (24.7%)	0.004

Figure S3. TWISST gene tree discordance summaries. Twenty trios were tested, using *M. aurantiacus* as the outgroup in all tests. Shown are the ten trios with significant

689 overrepresentation of one alternate topology over another (binomial test, expected ratio 1:1,
690 Bonferroni-corrected p_{corr}<0.05). For each trio, the number of genes support each topology are
691 given, along with the percentage of total trees. A total of 17,524 genes were used for all trios. J
692 = *M. johnstonii*, B = *M. brevipes,* F = *M. fremontii*, S = Sespe creek population, C = *M. constrictus*,
693 N = *M. nanus*, O = *M. aurantiacus* complex.
694

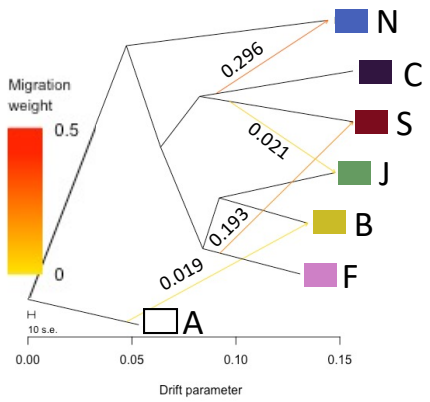

695
696 **Figure S4. TreeMix network analysis results for four migration edges.** The edge (C to N) was
697 selected in the network with a single edge, which was the best model according to OptM; other
698 edges improved the log-likelihood of the model by progressively decreasing amounts. Migration
699 weights for the four-edge model are provided next to each edge.
700

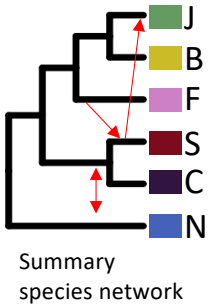

701
702 **Figure S5. Summary of best-supported introgression events from multiple methods.** Three
703 introgression events were supported by f_{branch} , TWISST, and TreeMix results. The exact identity
704 and direction of individual introgression events may be different due to shared ancestry and
705 incomplete sampling; for example, signatures of introgression from all of *M. fremontii, M.*
706 *johnstonii, and M. brevipes* into Sespe Creek may be caused by a single event in a common
707 ancestor, an unsampled relative, or just one of the sampled species.
708

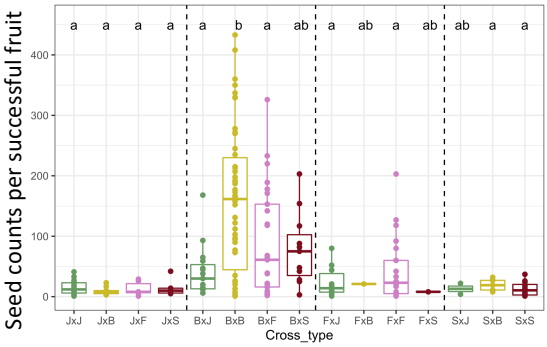

Figure S6. Seed counts do not indicate hybrid deficiency. Seed counts per fruit for fruits producing at least one seed. *M. brevipes* produces more seeds per fruit than the other species, but interspecific crosses do not show a reduction in seed count relative to intraspecific crosses. Letters indicate significance in post-hoc Tukey tests from a linear model; cross types sharing a letter are not significantly different.

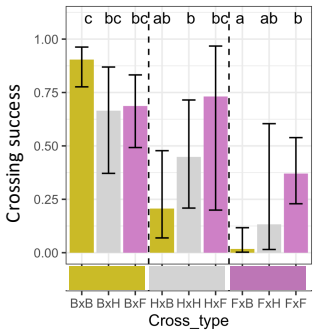

Figure S7. Crossing success in BxF hybrids is additive on maternal and paternal sides. Crossing success (probability of at least one seed produced from a cross) from crosses involving *M. brevipes* x *M. fremontii* F1 hybrids and their parental species. Shown are least-square means and asymptotic confidence intervals from a binomial GLMM. Letters indicate significance in post-hoc Tukey tests; cross types sharing a letter are not significantly different. HxB crosses have intermediate crossing success compared to BxB and FxB crosses (gold bars), indicating an additive effect of maternal species. Similarly, FxH crosses have intermediate crossing success compared to FxB and FxF crosses (right three bars), indicating an additive effect of paternal species. HxH have intermediate success compared to BxH and FxH (gray bars), as well as compared to HxB and HxF (middle three bars), further supporting additive patterns. B = *M. brevipes,* F = *M. fremontii*, H = F1 hybrids between *M. brevipes* and *M. fremontii*.

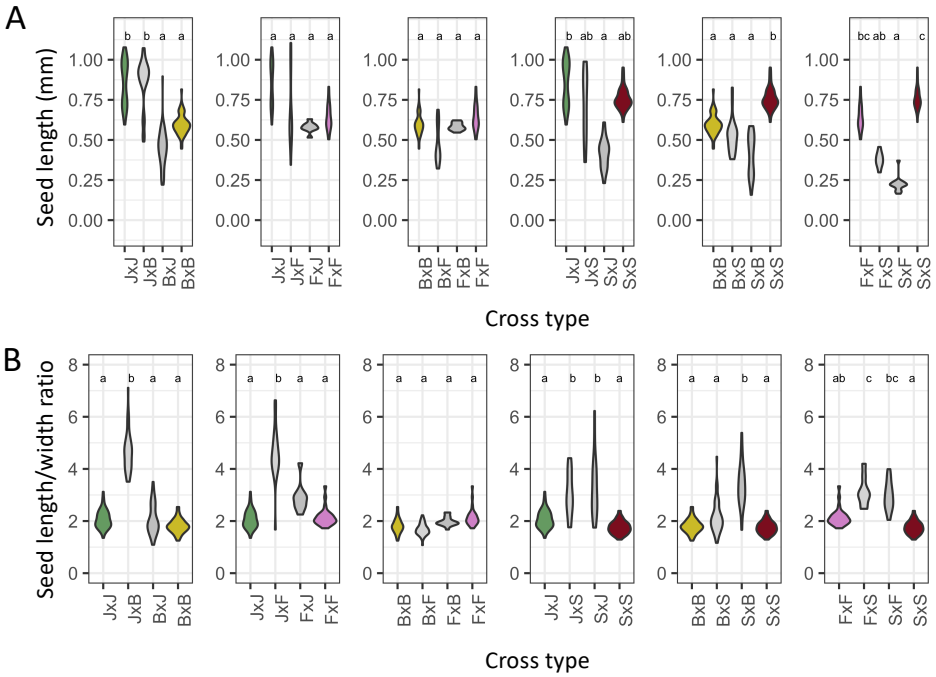

Figure S8. Seed measurements for all intra- and interspecific cross types. (A) Seed length and (B) length/width ratios. Violin plots show distribution of individual seeds. Letters indicate significance from post-hoc Tukey tests after running six independent species-pair models. One species pair had a significant reciprocal difference in hybrid seed size, while three pairs had a significant reciprocal difference in seed length/width ratio; length/width ratio was elevated compared to both parents for six cross types.

Table S1. Population location information and number of samples used per population.

Population	Species	Latitude	Longitude	Samples sequenced	Samples used in crosses† 1st gen	2nd gen
J31	*Mimulus johnstonii*	34.401950	-117.81580	5	9	7
B07	*Mimulus brevipes*	34.358990	-118.39803	3	14	1
B11	*Mimulus brevipes*	33.656155	-117.45298	6	13	7
B12	*Mimulus brevipes*	32.889920	-116.57440	4	23	2
B19	*Mimulus brevipes*	33.333300	-116.94200	4	33	20
F06	*Mimulus fremontii*	34.693000	-119.32900	2	9	--
F21	*Mimulus fremontii*	34.460560	-117.67316	3	11	--
F22	*Mimulus fremontii*	34.376390	-117.59682	2	6	--
S25	'Sespe Creek'	34.565773	-119.26081	2	3	3
N01	*Mimulus nanus*	42.638395	-118.57760	2	--	--
C01	*Mimulus constrictus*	34.798960	-119.00466	1	--	--

† 1st gen = wild-collected, 2nd gen = greenhouse-produced from hand pollination. All sequenced individuals were grown directly from wild-collected seeds, except the two *M. nanus* samples, which were collected from wild individuals.

Table S2. Sequencing and coverage information.

Sample info			Read pairs			Coverage per base	
Sample†	Pop	Batch	Raw	Aligned	%	All sites	% with >=4X coverage
BREV07_3_1	B07	1	47,522,461	13,277,523	27.9%	12.47	39.03%
BREV07_5_1	B07	1	49,800,600	15,174,402	30.5%	14.04	39.09%
BREV12_3_1	B12	1	49,704,577	15,840,128	31.9%	15.68	37.55%
BREV12_5_1	B12	1	49,785,466	14,465,999	29.1%	13.52	39.79%
BREV12_6_1	B19	1	49,555,797	15,518,193	31.3%	14.54	39.49%
BREV19_1_1	B19	1	49,652,489	16,050,274	32.3%	15.62	37.83%
FREM22_6_1	F22	1	49,332,251	8,451,160	17.1%	7.30	33.81%
JOHN31_5_1	J31	1	49,714,033	13,727,590	27.6%	12.82	37.51%
BREV07_6_1	B07	2	25,682,314	5,672,576	22.1%	5.67	32.30%
BREV11_5_3	B11	2	28,911,480	5,804,484	20.1%	5.35	31.82%
BREV12_4_1	B12	2	28,052,293	6,443,496	23.0%	6.28	33.38%
BREV19_2_1	B19	2	29,339,237	7,002,395	23.9%	6.87	33.83%
BREV19_3_1	B19	2	36,190,791	3,248,019	9.0%	3.10	21.10%
BREV19_4_1	B19	2	14,858,533	2,429,889	16.4%	2.19	16.18%
FREM06_3_2	F06	2	30,075,452	5,408,560	18.0%	4.51	26.45%
FREM06_4_3	F06	2	29,784,495	6,422,159	21.6%	5.68	29.74%
FREM21_2_1	F21	2	33,601,408	5,451,858	16.2%	4.60	27.10%
FREM22_5_1	F22	2	24,172,306	2,679,095	11.1%	2.35	19.37%
JOHN31_1_1	J31	2	47,347,007	6,441,313	13.6%	6.20	31.22%
JOHN31_2_1	J31	2	64,312,829	10,195,170	15.9%	9.88	36.43%
JOHN31_4_1	J31	2	23,147,570	3,938,270	17.0%	3.82	24.04%
JOHN31_5_2	J31	2	32,146,268	5,382,624	16.7%	4.86	25.48%
BREV11_1_11	B11	3	12,194,294	3,311,065	27.2%	3.16	18.64%
BREV11_3_4	B11	3	16,149,111	4,165,590	25.8%	3.88	24.46%
BREV11_5_1	B11	3	19,609,920	5,018,757	25.6%	4.72	26.70%
BREV11_6_11	B11	3	17,240,947	4,349,611	25.2%	4.02	26.63%
FREM21_3_11	F21	3	31,307,714	5,636,788	18.0%	4.86	30.25%
FREM21_4_11	F21	3	23,442,361	4,186,587	17.9%	3.67	24.90%
SESP25_1_1	S25	3	37,881,366	8,233,912	21.7%	7.70	34.70%
SESP25_1_2	S25	3	22,013,442	5,056,136	23.0%	4.58	29.93%
NANU01_1	N01	3	15,545,612	2,612,978	16.8%	2.26	14.32%
NANU01_2	N01	3	14,729,812	2,603,428	17.7%	2.38	17.61%

CONS01_1_1	C01	4	16,909,453	4,072,713	24.1%	4.10	16.6%
AURA_ari	AURA	SRX6077155	15,314,328	5,630,656	36.8%	7.14	64.06%
AURA_aur	AURA	SRX6077153	18,453,062	7,584,963	41.1%	10.02	75.92%
AURA_gra	AURA	SRX6077242	12,454,896	6,061,103	48.7%	7.84	66.98%
AURA_pun	AURA	SRX6077404	14,056,153	5,076,335	36.1%	6.53	60.90%
CLEV_cle	AURA	SRX6077240	12,810,520	4,567,552	35.7%	5.58	53.01%

† 1st number indicates population, 2nd number indicates maternal family, 3rd number refers to the individual plant. *M. nanus* samples (NANU01_1 and NANU01_2) are from distinct wild plants.

Table S3. Pedigree information for *M. brevipes* and *M. fremontii* F1 families.

				Number of individuals used		
Line name	Line type	Maternal	Paternal	Pollen viability	Maternal crosses	Paternal crosses
BF1	BxF F1 hybrid	B19_3_2	F6_4_3	0	1	1
BF2	BxF F1 hybrid	B12_5_2	F21_3_1	2	1	1
BF3	BxF F1 hybrid	B19_1_1	F6_3_1	7	7	6
BF5	BxF F1 hybrid	B19_4_14	F21_4_11	4	2	0

Table S4. Nucleotide diversity and divergence values at synonymous sites. Values were calculated using pixy for all individual pairwise comparisons, then averaged across comparisons within a group.

Species	Heterozygosity	Diversity
AUR	0.0025	0.0163
B	0.0198	0.0229
C	0.0135	--
F	0.0209	0.0316
J	0.0170	0.0174
N	0.0154	0.0324
S	0.0180	0.0178

Species 1	Species 2	Divergence
AUR	C	0.0940
AUR	N	0.0945
AUR	S	0.0991
AUR	B	0.1000
AUR	J	0.1005
AUR	F	0.1027
B	J	0.0525
B	F	0.0599

B	S	0.0697
B	C	0.0707
B	N	0.0830
C	S	0.0605
C	J	0.0702
C	F	0.0730
C	N	0.0753
F	J	0.0598
F	S	0.0715
F	N	0.0860
J	S	0.0692
J	N	0.0828
N	S	0.0791

Table S5. ABBA-BABA test results for the full 'filtered' SNP dataset.

P1	P2	P3	D	Z-score	Significance	*f4*-ratio	BBAA	ABBA	BABA
B	**J**	**F**	0.025	4.1	***	0.017	140199	101734	96787
B	**J**	**S**	0.077	14.5	***	0.023	225194	81493	69780
J	F	S	0.012	2.5	n.s.	0.004	193112	89515	87397
B	**F**	**S**	0.080	16.0	***	0.027	192818	93743	79920
B	**J**	**C**	0.060	12.4	***	0.015	217482	60440	53601
J	F	C	0.001	0.3	n.s.	0.000	190562	65810	65623
B	**F**	**C**	0.054	11.7	***	0.016	189827	68457	61448
C	**S**	**J**	0.193	38.6	***	0.072	128359	98268	66479
C	**S**	**F**	0.199	39.8	***	0.093	129273	101021	67419
C	**S**	**B**	0.186	35.9	***	0.077	133849	94966	65145
B	**J**	**N**	0.058	13.7	***	0.011	310955	59579	53098
F	**J**	**N**	0.027	8.0	***	0.006	281234	65746	62337
B	**F**	**N**	0.024	7.2	***	0.005	280189	64934	61873
J	**S**	**N**	0.091	24.8	***	0.027	184994	88233	73578
B	**S**	**N**	0.127	28.9	***	0.037	179236	92602	71726
F	**S**	**N**	0.110	28.9	***	0.032	190288	90971	73014
J	**C**	**N**	0.099	23.1	***	0.032	126808	82206	67332
B	**C**	**N**	0.131	25.7	***	0.042	124234	85599	65732
F	**C**	**N**	0.114	23.8	***	0.037	129720	84553	67229
S	**C**	**N**	0.036	7.9	***	0.010	166409	65159	60632

***p_{corr}<0.001, n.s.=not significant

Table S6. Crossing success and seed viability for each cross type.

Maternal species	Paternal species	Cross type	Crossing success (total crosses)	Seed viability (total seeds)
M. johnstonii	*M. johnstonii*	JxJ	0.538 (39)	0.745 (306)
M. johnstonii	*M. brevipes*	JxB	0.440 (25)	**0.000 (98)**
M. johnstonii	*M. fremontii*	JxF	0.600 (10)	**0.000 (78)**
M. johnstonii	Sespe Creek	JxS	0.600 (5)	**0.015 (66)**
M. brevipes	*M. johnstonii*	BxJ	0.484 (31)	**0.006 (630)**
M. brevipes	*M. brevipes*	BxB	0.902 (51)	0.981 (7292)
M. brevipes	*M. fremontii*	BxF	0.694 (36)	0.821 (2226)
M. brevipes	Sespe Creek	BxS	0.500 (6)	**0.018 (217)**
M. fremontii	*M. johnstonii*	FxJ	0.500 (20)	**0.012 (246)**
M. fremontii	*M. brevipes*	FxB	**0.017 (58)**	0.952 (21)
M. fremontii	*M. fremontii*	FxF	0.382 (55)	0.902 (911)
M. fremontii	Sespe Creek	FxS	0.091 (11)	**0.000 (8)**
Sespe Creek	*M. johnstonii*	SxJ	0.125 (8)	**0.000 (4)**
Sespe Creek	*M. brevipes*	SxB	0.333 (6)	**0.000 (38)**
Sespe Creek	*M. fremontii*	SxF	0.000 (4)	n/a (0)
Sespe Creek	Sespe Creek	SxS	0.409 (22)	0.909 (88)

Bolded values are significant in Tukey tests compared to both parental cross types.

REFERENCES

Aagaard, J. E., George, R. D., Fishman, L., MacCoss, M. J., & Swanson, W. J. (2013). Selection on Plant Male Function Genes Identifies Candidates for Reproductive Isolation of Yellow Monkeyflowers. *PLoS Genetics*, *9*(12). https://doi.org/10.1371/journal.pgen.1003965

Ascher, P. D., & Drewlow, L. W. (1975). The effect of prepollination injection with stigmatic exudate on interspecific pollen tube growth in Lilium longiflorum thunb. Styles. *Plant Science Letters*, *4*(6), 401–405. https://doi.org/10.1016/0304-4211(75)90269-2

Baack, E., Melo, M. C., Rieseberg, L. H., & Ortiz-Barrientos, D. (2015). The origins of reproductive isolation in plants. *New Phytologist*, *207*(4), 968–984. https://doi.org/10.1111/nph.13424

Baldwin, B. G., Goldman, D., Keil, D. J., Patterson, R., Rosatti, T. J., & Wilken, D. (Eds.). (2012). *The Jepson Manual: Vascular Plants of California, Thoroughly Revised and Expanded* (2nd ed.).

Barker, W. R. (Bill), Nesom, G. L., Beardsley, P. M., & Fraga, N. S. (2012). A taxonomic conspectus of phrymaceae: A narrowed circumscription for. *Phytoneuron*, *May*, 1–60.

Beardsley, P. M., Schoenig, S. E., Whittall, J. B., & Olmstead, R. G. (2004). Patterns of evolution in western North American Mimulus (Phrymaceae). *American Journal of Botany*, *91*(3), 474–489. https://doi.org/10.3732/ajb.91.3.474

Behm, J. E., Ives, A. R., & Boughman, J. W. (2010). Breakdown in postmating isolation and the collapse of a species pair through hybridization. *The American Naturalist*, *175*(1), 11–26. https://doi.org/10.1086/648559

Bernacchi, D., & Tanksley, S. D. (1997). An Interspecific Backcross of Lycopersicon esculentum × L. hirsutum: Linkage Analysis and a QTL Study of Sexual Compatibility Factors and Floral Traits. *Genetics*, *147*(2), 861–877. https://doi.org/10.1093/genetics/147.2.861

Bickford, D., Lohman, D. J., Sodhi, N. S., Ng, P. K. L., Meier, R., Winker, K., Ingram, K. K., & Das, I. (2007). Cryptic species as a window on diversity and conservation. *Trends in Ecology & Evolution*, *22*(3), 148–155. https://doi.org/10.1016/j.tree.2006.11.004

Bolger, A. M., Lohse, M., & Usadel, B. (2014). Trimmomatic: A flexible trimmer for Illumina sequence data. *Bioinformatics*, *30*(15), 2114–2120. https://doi.org/10.1093/bioinformatics/btu170

Bowers, J. E. (1982). The plant ecology of inland dunes in western North America. *Journal of Arid Environments*, *5*(3), 199–220. https://doi.org/10.1016/S0140-1963(18)31444-7

Brandvain, Y., & Haig, D. (2005). Divergent Mating Systems and Parental Conflict as a Barrier to Hybridization in Flowering Plants. *The American Naturalist*, *166*(3), 330–338. https://doi.org/10.1086/432036

Brandvain, Y., Kenney, A. M., Flagel, L., Coop, G., & Sweigart, A. L. (2014). Speciation and Introgression between Mimulus nasutus and Mimulus guttatus. *PLoS Genetics*, *10*(6), e1004410. https://doi.org/10.1371/journal.pgen.1004410

Broad Institute. (2019). *Picard Toolkit, GitHub repository*. https://broadinstitute.github.io/picard/

Christie, K., Fraser, L. S., & Lowry, D. B. (2022). The strength of reproductive isolating barriers in seed plants: Insights from studies quantifying premating and postmating reproductive barriers over the past 15 years. *Evolution*, evo.14565. https://doi.org/10.1111/evo.14565

Christie, K., & Strauss, S. Y. (2018). Along the speciation continuum: Quantifying intrinsic and extrinsic isolating barriers across five million years of evolutionary divergence in California jewelflowers. *Evolution*, *72*(5), 1063–1079. https://doi.org/10.1111/evo.13477

809 Coughlan, J. M., & Matute, D. R. (2020). The importance of intrinsic postzygotic barriers
810 throughout the speciation process: Intrinsic barriers throughout speciation.
811 *Philosophical Transactions of the Royal Society B: Biological Sciences*, *375*(1806).
812 https://doi.org/10.1098/rstb.2019.0533
813 Coughlan, J. M., Wilson Brown, M., & Willis, J. H. (2020). Patterns of Hybrid Seed Inviability in
814 the Mimulus guttatus sp. Complex Reveal a Potential Role of Parental Conflict in
815 Reproductive Isolation. *Current Biology*, *30*(1), 83-93.e5.
816 https://doi.org/10.1016/j.cub.2019.11.023
817 Coyne, J. A., & Orr, H. A. (1989). Patterns of Speciation in Drosophila. *Evolution*, *43*(2), 362–381.
818 Coyne, J. A., & Orr, H. A. (1997). Patterns of Speciation in Drosophila Revisited. *Evolution*, *51*(1),
819 295. https://doi.org/10.2307/2410984
820 Crespi, B., & Nosil, P. (2013). Conflictual speciation: Species formation via genomic conflict.
821 *Trends in Ecology & Evolution*, *28*(1), 48–57. https://doi.org/10.1016/j.tree.2012.08.015
822 Curtu, A. L., Gailing, O., & Finkeldey, R. (2009). Patterns of contemporary hybridization inferred
823 from paternity analysis in a four-oak-species forest. *BMC Evolutionary Biology*, *9*(1), 284.
824 https://doi.org/10.1186/1471-2148-9-284
825 Danecek, P., Bonfield, J. K., Liddle, J., Marshall, J., Ohan, V., Pollard, M. O., Whitwham, A.,
826 Keane, T., McCarthy, S. A., Davies, R. M., & Li, H. (2021). Twelve years of SAMtools and
827 BCFtools. *GigaScience*, *10*(2), giab008. https://doi.org/10.1093/gigascience/giab008
828 D'Angiolo, M., De Chiara, M., Yue, J.-X., Irizar, A., Stenberg, S., Persson, K., Llored, A., Barré, B.,
829 Schacherer, J., Marangoni, R., Gilson, E., Warringer, J., & Liti, G. (2020). A yeast living

830 ancestor reveals the origin of genomic introgressions. *Nature*, *587*(7834), Article 7834.
831 https://doi.org/10.1038/s41586-020-2889-1
832 Darwin, C. (1859). *On the origin of species by means of natural selection*. John Murray.
833 http://darwin-online.org.uk/converted/pdf/1861_OriginNY_F382.pdf
834 Ferris, K. G., Sexton, J. P., & Willis, J. H. (2014). Speciation on a local geographic scale: The
835 evolution of a rare rock outcrop specialist in *Mimulus*. *Philosophical Transactions of the*
836 *Royal Society B: Biological Sciences*, *369*(1648), 20140001.
837 https://doi.org/10.1098/rstb.2014.0001
838 Fishman, L. (2020). *96-well CTAB-chloroform DNA extraction*. protocols.io.
839 https://dx.doi.org/10.17504/protocols.io.bgv6jw9e
840 Fishman, L., Aagaard, J., & Tuthill, J. C. (2008). Toward the Evolutionary Genomics of
841 Gametophytic Divergence: Patterns of Transmission Ratio Distortion in Monkeyflower
842 (mimulus) Hybrids Reveal a Complex Genetic Basis for Conspecific Pollen Precedence.
843 *Evolution*, *62*(12), 2958–2970. https://doi.org/10.1111/j.1558-5646.2008.00475.x
844 Fishman, L., Sweigart, A. L., Kenney, A. M., & Campbell, S. (2014). Major quantitative trait loci
845 control divergence in critical photoperiod for flowering between selfing and outcrossing
846 species of monkeyflower (Mimulus). *New Phytologist*, *201*(4), 1498–1507.
847 https://doi.org/10.1111/nph.12618
848 Fishman, L., & Willis, J. H. (2006). A cytonuclear incompatibility causes anther sterility in
849 Mimulus hybrids. *Evolution*, *60*(7), 1372–1381. https://doi.org/10.1111/j.0014-
850 3820.2006.tb01216.x

Fitak, R. R. (2021). OptM: Estimating the optimal number of migration edges on population trees using Treemix. *Biology Methods and Protocols*, *6*(1), bpab017. https://doi.org/10.1093/biomethods/bpab017

Fujii, S., Tsuchimatsu, T., Kimura, Y., Ishida, S., Tangpranomkorn, S., Shimosato-Asano, H., Iwano, M., Furukawa, S., Itoyama, W., Wada, Y., Shimizu, K. K., & Takayama, S. (2019). A stigmatic gene confers interspecies incompatibility in the Brassicaceae. *Nature Plants*, *5*(7), Article 7. https://doi.org/10.1038/s41477-019-0444-6

Gore, P., Potts, B., Volker, P., & Megalos, J. (1990). Unilateral Cross-Incompatibility in Eucalyptus: The Case of Hybridisation Between E. globulus and E. nitens. *Australian Journal of Botany*, *38*(4), 383. https://doi.org/10.1071/BT9900383

Goulet, B. E., Roda, F., & Hopkins, R. (2017). Hybridization in plants: Old ideas, new techniques. *Plant Physiology*, *173*(1), 65–78. https://doi.org/10.1104/pp.16.01340

Grant, A. L. (1924). A Monograph of the Genus Mimulus. *Annals of the Missouri Botanical Garden*, *11*(2/3), 99–388. https://doi.org/10.2307/2394024

Grant, V. (1981). *Plant Speciation*. Columbia University Press.

Green, R. E., Krause, J., Briggs, A. W., Maricic, T., Stenzel, U., Kircher, M., Patterson, N., Li, H., Zhai, W., Fritz, M. H.-Y., Hansen, N. F., Durand, E. Y., Malaspinas, A.-S., Jensen, J. D., Marques-Bonet, T., Alkan, C., Prüfer, K., Meyer, M., Burbano, H. A., … Pääbo, S. (2010). A draft sequence of the Neandertal genome. *Science (New York, N.Y.)*, *328*(5979), 710–722. https://doi.org/10.1126/science.1188021

871 Guerrero, R. F., Muir, C. D., Josway, S., & Moyle, L. C. (2017). Pervasive antagonistic interactions
872 among hybrid incompatibility loci. *PLOS Genetics*, *13*(6), e1006817.
873 https://doi.org/10.1371/journal.pgen.1006817
874 Haig, D., & Westoby, M. (1991). Genomic imprinting in endosperm: Its effect on seed
875 development in crosses between species, and between different ploidies of the same
876 species, and its implications for the evolution of apomixis. *Philosophical Transactions -*
877 *Royal Society of London, B*, *333*, 1–13.
878 Hamlin, J. A. P., Hibbins, M. S., & Moyle, L. C. (2020). Assessing biological factors affecting
879 postspeciation introgression. *Evolution Letters*, *4*(2), 137–154.
880 https://doi.org/10.1002/evl3.159
881 Hogenboom, N. G., Mather, K., Heslop-Harrison, J., & Lewis, D. (1975). Incompatibility and
882 incongruity: Two different mechanisms for the non-functioning of intimate partner
883 relationships. *Proceedings of the Royal Society of London. Series B. Biological Sciences*,
884 *188*(1092), 361–375. https://doi.org/10.1098/rspb.1975.0025
885 Kay, K. M., Woolhouse, S., Smith, B. A., Pope, N. S., & Rajakaruna, N. (2018). Sympatric
886 serpentine endemic Monardella (Lamiaceae) species maintain habitat differences
887 despite hybridization. *Molecular Ecology*, *27*(9), 2302–2316.
888 https://doi.org/10.1111/mec.14582
889 Kenney, A. M., & Sweigart, A. L. (2016). Reproductive isolation and introgression between
890 sympatric Mimulus species. *Molecular Ecology*, *25*(11), 2499–2517.
891 https://doi.org/10.1111/mec.13630

Kleindorfer, S., O'Connor, J. A., Dudaniec, R. Y., Myers, S. A., Robertson, J., & Sulloway, F. J. (2014). Species collapse via hybridization in Darwin's tree finches. *The American Naturalist*, *183*(3), 325–341. https://doi.org/10.1086/674899

Koch, M. A., Haubold, B., & Mitchell-Olds, T. (2000). Comparative Evolutionary Analysis of Chalcone Synthase and Alcohol Dehydrogenase Loci in Arabidopsis, Arabis, and Related Genera (Brassicaceae). *Molecular Biology and Evolution*, *17*(10), 1483–1498. https://doi.org/10.1093/oxfordjournals.molbev.a026248

Korunes, K. L., & Samuk, K. (2021). pixy: Unbiased estimation of nucleotide diversity and divergence in the presence of missing data. *Molecular Ecology Resources*, *21*(4), 1359–1368. https://doi.org/10.1111/1755-0998.13326

Kryvokhyzha, D. (n.d.). *GATK: The best practice for genotype calling in a non-model organism*. Dmytro Kryvokhyzha - Bioinformatics & Genomics Scientist. Retrieved August 8, 2022, from https://evodify.com/gatk-in-non-model-organism/

Kuboyama, T., Chung, C. S., & Takeda, G. (1994). The diversity of interspecific pollen-pistil incongruity in Nicotiana. *Sexual Plant Reproduction*, *7*(4), 250–258. https://doi.org/10.1007/BF00232744

Lafon-Placette, C., Johannessen, I. M., Hornslien, K. S., Ali, M. F., Bjerkan, K. N., Bramsiepe, J., Glöckle, B. M., Rebernig, C. A., Brysting, A. K., Grini, P. E., & Köhler, C. (2017). Endosperm-based hybridization barriers explain the pattern of gene flow between Arabidopsis lyrata and Arabidopsis arenosa in Central Europe. *Proceedings of the National Academy of Sciences*, *114*(6), E1027–E1035. https://doi.org/10.1073/pnas.1615123114

Lafon-Placette, C., & Köhler, C. (2016). Endosperm-based postzygotic hybridization barriers: Developmental mechanisms and evolutionary drivers. *Molecular Ecology*, *25*(11), 2620–2629. https://doi.org/10.1111/mec.13552

Le Gac, M., Hood, M. E., & Giraud, T. (2007). Evolution of Reproductive Isolation Within a Parasitic Fungal Species Complex. *Evolution*, *61*(7), 1781–1787. https://doi.org/10.1111/j.1558-5646.2007.00144.x

Leishman, M., Wright, I., Moles, A., & Westoby, M. (2000). The Evolutionary Ecology of Seed Size. *Seeds: The Ecology of Regeneration in Plant Communities*, *2*. https://doi.org/10.1079/9780851994321.0031

Li, H. (2018). *Seqtk* (1.3). https://github.com/lh3/seqtk

Li, H., & Durbin, R. (2009). Fast and accurate short read alignment with Burrows-Wheeler transform. *Bioinformatics*, *25*(14), 1754–1760. https://doi.org/10.1093/bioinformatics/btp324

Lowry, D. B., Sobel, J. M., Angert, A. L., Ashman, T.-L., Baker, R. L., Blackman, B. K., Brandvain, Y., Byers, K. J. R. P., Cooley, A. M., Coughlan, J. M., Dudash, M. R., Fenster, C. B., Ferris, K. G., Fishman, L., Friedman, J., Grossenbacher, D. L., Holeski, L. M., Ivey, C. T., Kay, K. M., … Yuan, Y.-W. (2019). The case for the continued use of the genus name Mimulus for all monkeyflowers. *TAXON*, *68*(4), 617–623. https://doi.org/10.1002/tax.12122

Lowry, D. B., & Willis, J. H. (2010). A widespread chromosomal inversion polymorphism contributes to a major life-history transition, local adaptation, and reproductive isolation. *PLoS Biology*, *8*(9). https://doi.org/10.1371/journal.pbio.1000500

Malinsky, M., Matschiner, M., & Svardal, H. (2021). Dsuite—Fast D-statistics and related admixture evidence from VCF files. *Molecular Ecology Resources*, *21*(2), 584–595. https://doi.org/10.1111/1755-0998.13265

Mallet, J., Beltrán, M., Neukirchen, W., & Linares, M. (2007). Natural hybridization in heliconiine butterflies: The species boundary as a continuum. *BMC Evolutionary Biology*, *7*(1), 28. https://doi.org/10.1186/1471-2148-7-28

Malone, J. H., & Fontenot, B. E. (2008). Patterns of Reproductive Isolation in Toads. *PLoS ONE*, *3*(12), e3900. https://doi.org/10.1371/journal.pone.0003900

Martin, S. H., & Van Belleghem, S. M. (2017). Exploring Evolutionary Relationships Across the Genome Using Topology Weighting. *Genetics*, *206*(1), 429–438. https://doi.org/10.1534/genetics.116.194720

Matute, D. R., & Cooper, B. S. (2021). Comparative studies on speciation: 30 years since Coyne and Orr. *Evolution*, *1989*, 1–15. https://doi.org/10.1111/evo.14181

Moyle, L. C., Olson, M. S., & Tiffin, P. (2004). Patterns of reproductive isolation in three angiosperm genera. *Evolution*, *58*(6), 1195–1208. https://doi.org/10.1111/j.0014-3820.2004.tb01700.x

Moyle, L. C., & Payseur, B. A. (2009). Reproductive isolation grows on trees. *Trends in Ecology & Evolution*, *24*(11), 591–598. https://doi.org/10.1016/j.tree.2009.05.010

Nelson, T. C., Stathos, A. M., Vanderpool, D. D., Finseth, F. R., Yuan, Y., & Fishman, L. (2021). Ancient and recent introgression shape the evolutionary history of pollinator adaptation and speciation in a model monkeyflower radiation (Mimulus section Erythranthe). *PLoS Genetics*, *17*(2), e1009095. https://doi.org/10.1371/journal.pgen.1009095

Nesom, G. L. (2013). Taxonomic notes on Diplacus (Phrymaceae). *Phytoneuron*, 8.

Oneal, E., Willis, J. H., & Franks, R. G. (2016). Disruption of endosperm development is a major cause of hybrid seed inviability between *Mimulus guttatus* and *Mimulus nudatus*. *New Phytologist*, *210*(3), 1107–1120. https://doi.org/10.1111/nph.13842

Pickrell, J. K., & Pritchard, J. K. (2012). Inference of Population Splits and Mixtures from Genome-Wide Allele Frequency Data. *PLOS Genetics*, *8*(11), e1002967. https://doi.org/10.1371/journal.pgen.1002967

Presgraves, D. C. (2002). Patterns of Postzygotic Isolation in Lepidoptera. *Evolution*, *56*(6), 1168–1183. https://doi.org/10.1111/j.0014-3820.2002.tb01430.x

Rabiee, M., Sayyari, E., & Mirarab, S. (2019). Multi-allele species reconstruction using ASTRAL. *Molecular Phylogenetics and Evolution*, *130*, 286–296. https://doi.org/10.1016/j.ympev.2018.10.033

Ramsey, J., Bradshaw, H. D., & Schemske, D. W. (2003). Components of reproductive isolation between the monkeyflowers Mimulus lewisii and M. cardinalis (Phrymaceae). *Evolution*, *57*(7), 1520–1534. https://doi.org/10.1111/j.0014-3820.2003.tb00360.x

Raunsgard, A., Opedal, Ø. H., Ekrem, R. K., Wright, J., Bolstad, G. H., Armbruster, W. S., & Pélabon, C. (2018). Intersexual conflict over seed size is stronger in more outcrossed populations of a mixed-mating plant. *Proceedings of the National Academy of Sciences*, *115*(45), 11561–11566. https://doi.org/10.1073/pnas.1810979115

Rebernig, C. A., Lafon-Placette, C., Hatorangan, M. R., Slotte, T., & Köhler, C. (2015). Non-reciprocal Interspecies Hybridization Barriers in the Capsella Genus Are Established in

the Endosperm. *PLOS Genetics*, *11*(6), e1005295. https://doi.org/10.1371/journal.pgen.1005295

Roda, F., & Hopkins, R. (2019). Correlated evolution of self and interspecific incompatibility across the range of a Texas wildflower. *New Phytologist*, *221*(1), 553–564. https://doi.org/10.1111/nph.15340

Roth, M., Florez-Rueda, A. M., & Städler, T. (2019). Differences in Effective Ploidy Drive Genome-Wide Endosperm Expression Polarization and Seed Failure in Wild Tomato Hybrids. *Genetics*, *212*(1), 141–152. https://doi.org/10.1534/genetics.119.302056

Rushworth, C. A., Wardlaw, A. M., Ross-Ibarra, J., & Brandvain, Y. (2022). Conflict over fertilization underlies the transient evolution of reinforcement. *PLOS Biology*, *20*(10), e3001814. https://doi.org/10.1371/journal.pbio.3001814

Sackton, T. (2022). *Natural selection constrains neutral diversity across a wide range of species* [R]. https://github.com/tsackton/linked-selection/blob/da62043544dce9c9342f0a393f41c63bec292fcf/misc_scripts/Identify_4D_Sites.pl (Original work published 2014)

Sandstedt, G. D., & Sweigart, A. L. (2022). Developmental evidence for parental conflict in driving Mimulus species barriers. *New Phytologist*, *236*(4), 1545–1557. https://doi.org/10.1111/nph.18438

Sandstedt, G. D., Wu, C. A., & Sweigart, A. L. (2020). Evolution of multiple postzygotic barriers between species of the Mimulus tilingii complex. *Evolution*, *75*, 600–613. https://doi.org/10.1111/evo.14105

Scascitelli, M., Whitney, K. D., Randell, R. A., King, M., Buerkle, C. A., & Rieseberg, L. H. (2010). Genome scan of hybridizing sunflowers from Texas (Helianthus annuus and H. debilis) reveals asymmetric patterns of introgression and small islands of genomic differentiation. *Molecular Ecology*, *19*(3), 521–541. https://doi.org/10.1111/j.1365-294X.2009.04504.x

Schliep, K. P. (2011). phangorn: Phylogenetic analysis in R. *Bioinformatics*, *27*(4), 592–593. https://doi.org/10.1093/bioinformatics/btq706

Schumer, M., Xu, C., Powell, D. L., Durvasula, A., Skov, L., Holland, C., Blazier, J. C., Sankararaman, S., Andolfatto, P., Gil, †, Rosenthal, G., & Przeworski, M. (2018). Natural selection interacts with recombination to shape the evolution of hybrid genomes. *Science*, *360*(6389), 656–660.

Schwarzbach, A. E., Donovan, L. A., & Rieseberg, L. H. (2001). Transgressive character expression in a hybrid sunflower species. *American Journal of Botany*, *88*(2), 270–277. https://doi.org/10.2307/2657018

Scopece, G., Musacchio, A., Widmer, A., & Cozzolino, S. (2007). Patterns of reproductive isolation in Mediterranean deceptive orchids. *Evolution*, *61*(11), 2623–2642. https://doi.org/10.1111/j.1558-5646.2007.00231.x

Servedio, M. R., & Hermisson, J. (2020). The evolution of partial reproductive isolation as an adaptive optimum. *Evolution*, *74*(1), 4–14. https://doi.org/10.1111/evo.13880

Skogsmyr, I., & Lankinen, Å. (2002). Sexual selection: An evolutionary force in plants? *Biological Reviews*, *77*(4), 537–562. https://doi.org/10.1017/S1464793102005973

1020 Sobel, J. M. (2010). *Speciation in the western North American wildflower genus Mimulus* [Ph.D.,
1021 Michigan State University].
1022 https://www.proquest.com/docview/873378456/abstract/950327CDE46D4690PQ/1
1023 Sobel, J. M. (2014). Ecogeographic Isolation and Speciation in the Genus Mimulus. *The*
1024 *American Naturalist*, *184*(5), 565–579. https://doi.org/10.1086/678235
1025 Sobel, J. M., & Chen, G. F. (2014). Unification of methods for estimating the strength of
1026 reproductive isolation. *Evolution*, *68*(5), 1511–1522. https://doi.org/10.1111/evo.12362
1027 Stamatakis, A. (2014). RAxML version 8: A tool for phylogenetic analysis and post-analysis of
1028 large phylogenies. *Bioinformatics*, *30*(9), 1312–1313.
1029 https://doi.org/10.1093/bioinformatics/btu033
1030 Stankowski, S., Chase, M. A., Fuiten, A. M., Rodrigues, M. F., Ralph, P. L., & Streisfeld, M. A.
1031 (2019). Widespread selection and gene flow shape the genomic landscape during a
1032 radiation of monkeyflowers. *PLOS Biology*, *17*(7), e3000391.
1033 https://doi.org/10.1371/journal.pbio.3000391
1034 Stathos, A., & Fishman, L. (2014). Chromosomal rearrangements directly cause underdominant
1035 F1 pollen sterility in Mimulus lewisii–Mimulus cardinalis hybrids. *Evolution*, *68*(11),
1036 3109–3119. https://doi.org/10.1111/evo.12503
1037 Streisfeld, M. A., & Kohn, J. R. (2005). Contrasting patterns of floral and molecular variation
1038 across a cline in Mimulus aurantiacus. *Evolution*, *59*(12), 2548–2559.
1039 https://doi.org/10.1111/j.0014-3820.2005.tb00968.x
1040 Streisfeld, M. A., & Rausher, M. D. (2009). Altered trans-Regulatory Control of Gene Expression
1041 in Multiple Anthocyanin Genes Contributes to Adaptive Flower Color Evolution in

1042 Mimulus aurantiacus. *Molecular Biology and Evolution*, *26*(2), 433–444.
1043 https://doi.org/10.1093/molbev/msn268
1044 Struck, T. H., Feder, J. L., Bendiksby, M., Birkeland, S., Cerca, J., Gusarov, V. I., Kistenich, S.,
1045 Larsson, K.-H., Liow, L. H., Nowak, M. D., Stedje, B., Bachmann, L., & Dimitrov, D. (2018).
1046 Finding Evolutionary Processes Hidden in Cryptic Species. *Trends in Ecology & Evolution*,
1047 *33*(3), 153–163. https://doi.org/10.1016/j.tree.2017.11.007
1048 Sweigart, A. L., Fishman, L., & Willis, J. H. (2006). A simple genetic incompatibility causes hybrid
1049 male sterility in mimulus. *Genetics*, *172*(4), 2465–2479.
1050 https://doi.org/10.1534/genetics.105.053686
1051 Takeuchi, H., & Higashiyama, T. (2012). A Species-Specific Cluster of Defensin-Like Genes
1052 Encodes Diffusible Pollen Tube Attractants in Arabidopsis. *PLOS Biology*, *10*(12),
1053 e1001449. https://doi.org/10.1371/journal.pbio.1001449
1054 Tovar-Méndez, A., Kumar, A., Kondo, K., Ashford, A., Baek, Y. S., Welch, L., Bedinger, P. A., &
1055 McClure, B. A. (2014). Restoring pistil-side self-incompatibility factors recapitulates an
1056 interspecific reproductive barrier between tomato species. *Plant Journal*, *77*(5), 727–
1057 736. https://doi.org/10.1111/tpj.12424
1058 Van der Auwera, G., & O'Connor, B. (2020). *Genomics in the Cloud: Using Docker, GATK, and*
1059 *WDL in Terra (1st Edition)*. O'Reilly Media.
1060 Wheeler, M. J., Franklin-Tong, V. E., & Franklin, F. C. H. (2001). The molecular and genetic basis
1061 of pollen–pistil interactions. *New Phytologist*, *151*(3), 565–584.
1062 https://doi.org/10.1046/j.0028-646x.2001.00229.x

1063 Williams, E., & Rouse, J. (1988). Disparate Style Lengths Contribute to Isolation of Species in
1064 Rhododendron. *Australian Journal of Botany*, *36*(2), 183.
1065 https://doi.org/10.1071/BT9880183
1066 Xiong, T., & Mallet, J. (2022). On the impermanence of species: The collapse of genetic
1067 incompatibilities in hybridizing populations. *Evolution*, *76*(11), 2498–2512.
1068 https://doi.org/10.1111/evo.14626
1069 Yuan, Y.-W. (2019). Monkeyflowers (Mimulus): New model for plant developmental genetics
1070 and evo-devo. *New Phytologist*, *222*(2), 694–700. https://doi.org/10.1111/nph.15560
1071 Yuan, Y.-W., Sagawa, J. M., Young, R. C., Christensen, B. J., & Bradshaw, H. D., Jr. (2013). Genetic
1072 Dissection of a Major Anthocyanin QTL Contributing to Pollinator-Mediated
1073 Reproductive Isolation Between Sister Species of Mimulus. *Genetics*, *194*(1), 255–263.
1074 https://doi.org/10.1534/genetics.112.146852
1075 Zuellig, M. P., & Sweigart, A. L. (2018). A two-locus hybrid incompatibility is widespread,
1076 polymorphic, and active in natural populations of Mimulus. *Evolution*, *72*(11), 2394–
1077 2405. https://doi.org/10.1111/evo.13596
1078